African Journal of Pure and Applied Chemistry

ABOUT AJPAC

The **African Journal of Pure and Applied Chemistry (AJPAC)** is an open access journal that publishes research analysis and inquiry into issues of importance to the science community. Articles in AJPAC examine emerging trends and concerns in the areas of theoretical chemistry (quantum chemistry), supramolecular and macromolecular chemistry, relationships between chemistry and environment, and chemicals and medicine, organometallic compounds and complexes, chemical synthesis and properties, chemicals and biological matters, polymer synthesis and properties, nanomaterials and nanosystems, electrochemistry and biosensors, chemistry and industry, chemistry and biomaterials, advances in chemical analysis, instrumentation, speciation, bioavailability. The goal of AJPAC is to broaden the knowledge of scientists and academicians by promoting free access and provide valuable insight to chemistry-related information, research and ideas. AJPAC is a bimonthly publication and all articles are peer-reviewed.

African Journal of Pure and Applied Chemistry (AJPAC) is published twice a month (one volume per year) by Academic Journals.

Contact Us

Editorial Office:	ajpac@academicjournals.org
Help Desk:	helpdesk@academicjournals.org
Website:	http://www.academicjournals.org/journal/AJPAC
Submit manuscript online	http://ms.academicjournals.me/.

Editors

Prof. Tebello Nyokong
Acting Editor
Chemistry Department
Rhodes University
Grahamstown 6140,
South Africa.

Prof. F. Tafesse
Associate Editor
Associate professor
Inorganic chemistry
University of South Africa
South Africa.

African Journal of Pure and Applied Chemistry

ARTICLES

Full Length Research Paper

Biosynthesis of silver nanoparticles using *Garcinia kola* and its antimicrobial potential

Labulo Ayomide Hassan[1]*, Adesuji Temitope Elijah[1], Oseghale Charles Ojiefoh[1], Omojola Joseph[2], Bodede Olusola Sunday[3], Dare Enock Olugbenga[1,4] and Akinsiku Abimbola Anuoluwapo[5]

[1]Department of Chemistry, Federal University of Lafia, Lafia, Nasarawa State, Nigeria.
[2]Department of Physics, Federal University Lafia, Lafia, Nasarawa State, Nigeria.
[3]Department of Chemistry, College of Agriculture, Engineering and Science, University of Kwazulu- Natal, South Africa.
[4]Deparment of Chemistry Federal University of Agriculture, Abeokuta, Ogun State, Nigeria.
[5]Chemistry Department, Covenant University, Ota, Ogun State, Nigeria.

We have investigated the green synthesis and antimicrobial activity of silver nanoparticles using *Garcinia kola*. Aqueous extract of *G. kola* was used to reduce $AgNO_3$ solution to obtain black nanocrystal of silver nanoparticles. Antimicrobial activity of the silver nanoparticles was tested against *Escherichia coli, Klebsiella pneumonia, Bacillus subtilis, Staphylococcus aureus, Aspergillus niger, Rhizopus stolonifer* and *Candida albican*. The synthesized silver nanoparticles was characterized using UV-vis spectroscopy, X-ray diffraction (XRD), Transmission electron microscopy (TEM), and Fourier transform infrared (FTIR) spectroscopy. UV-visible exhibits prominently the characteristic surface plasmon resonance at around 427 nm. A remarkable particle growth onset of 10 min was observed while the reaction ended within 30 min. The XRD analysis shows that the synthesized silver nanoparticles are crystalline in nature and well-dispersed silver nanoparticles with an approximate size of 10.4 nm were observed on TEM. The synthesized silver was found to possess good antimicrobial activity against all the tested microbes. The application of the green synthesized nanoparticles can be used in many fields such as foods, beverages, cosmetics and medicine.

Key words: Silver, nanoparticles, green synthesis, *Garcinia kola* seed extract, transmission electron microscopy, antimicrobial activity.

INTRODUCTION

Nanotechnology is a growing field that has drawn the attention of researchers in different disciplines. Metal nanoparticles with controlled size and shape form the basis for advanced functional materials for electronic, sensor, optical devices (Gurunathan et al., 2009). Metal nanoparticles synthesis is achieved majorly using physical, chemical and biological approaches. Laser ablation (Tsuji et al., 2003), Arc discharged method (Tien

et al., 2008), irradiation (Yong et al., 1999), polyol process (Sun and Xia, 2002), polymers (Hebeish et al., 2011; Chengcai et al., 2005; Narendra and Khanna, 2007), co-precipitation (Yang et al., 2003), sol-gel (Lu et al., 2002), bacteria (Korbekandi et al., 2012), fungi (Ahmad et al., 2003; Balaji et al., 2009) have been used in the synthesis of nanoparticles. The use of plant extracts, enzymes, microorganisms, polymers, sugars and vitamins in nanoparticles formation has made nanotechnology a promising area of research (Oxana et al., 2013). Among the noble metals (e.g., Ag, Pt, Au and Pd), silver (Ag) is the metal of choice for potential applications in the field of biological systems, living organisms and medicine (Jain et al., 2009). The use of plant extract in synthesizing silver nanoparticles is eco-friendly, energy saving and can be easily scaled up. Biologically synthesized silver nanoparticles using medicinal plants or plant extracts include locust bean gum (Chandrakant et al., 2013), *Andrographis paniculata* (Venkata et al., 2014), lingonberry and cranberry juices (Judita et al., 2014), *Morinda citrifolia* (Gnanasekar et al., 2012), *Alternanthera dentata* (Deenadayalan et al., 2014), guava leaves extract (Shinde et al., 2014), *Gardenia jasminoides* (Lü et al., 2014), Jatropha seedcake (Anjali et al., 2013), *Mimusops elengi* (Hoskote et al., 2014), *Abutilon indicum* (Ashokkumar et al., 2015), *Ziziphora tenuior* (Babak and Gholamhoseinpoor, 2015), *Ficus carica* (Bulent et al., 2015), *Acacia auriculiformis* (Pradnya et al., 2014), *Cocos nucifera* (Mariselvama et al., 2014). Pineapple leave extract has also been used for the green synthesis of silver nanoparticles and its high antibacterial activities have been reported (Elemike et al., 2014). Recently our research group studied the growth kinetic of silver nanoparticles under the influence of plant biodiversity (Dare et al., 2015) for pharmaceutical and biological applications have been reported. *G. kola* Heckel (Clusiaceae), commonly known as bitter kola (English) and orogbo (Yoruba) is a widespread tree of evergreen forest valued in Nigeria for its medicinal nuts which has led to its exploitation in the natural forests in recent times (Ibikunle and Emmanuel, 2011). The phytochemicals obtained from *G. kola* as documented in literature include biflavonoids such as kolaflavonone, and 2 hydroxyflavonoids, xanthones, kolanone, ameakoflavone, 2,4-methylenecyclartenol, coumarine and prenylatebenzophenones, oleoresin, the chromanols, garcioic and garcinal (Adesuyi et al., 2012). Others are tannin, saponins, alkaloids, and cardiac glycoside. The proximate analyses showed that the sample has high level of carbohydrate, little amount of crude fibre and protein respectively and negligible amount of ash content and crude fat. This composition shows that the sample could be a good source of carbohydrate, dietary fibre and protein (He et al., 2007). Biomolecules with carbonyl, hydroxyl, and amine functional groups have the potential for metal ion reduction and capping the newly formed particles during their growth processes (Adesuyi et al.,

2012). In this work, we report a simple, nontoxic, and eco-friendly green synthesis of silver nanoparticles using aqueous seed extract of *G. kola* and no toxic chemicals are used as reducing and stabilizing agent during the synthesis.

METHODOLOGY

Materials

G. kola seeds and Silver nitrate ($AgNO_3$) of analytical grade was purchased from Sigma–Aldrich.

Organisms

Escherichia coli (*E. coli*), *Klebsiella pneumoniae* (*K. pneumoniae*), *Bacillus subtilis* (*B. subtilis*), *Staphylococcus aureus* (*S. aureus*), *Aspergillus niger* (*A. niger*), *Rhizophus stolonifer* (*R. stolonifer*), and *Candida albican* were collected at the Department of Microbiology, University of Ibadan.

Plants and preparation of extract

G. kola seeds were obtained from the local market in Lafia, the capital of Nasarawa State, Nigeria. 10 g of seeds was milled using an ordinary coffee grinder and ground kernel were boiled with 100 mL triply distilled/ deionized water for 10 min. After filtration through Whatman No 1, filter clear seed extract was obtained for further use. All the aqueous solutions were prepared using triply distilled deionized water and stored at 4°C for further use.

Synthesis of silver nanoparticles

10 ml of aqueous seed extract was added to 40 ml of 1 mM aqueous silver nitrate solution; the mixture was heated at 70°C in time intervals ranging from 2 to 30 min. Reduction of the Ag^+ ions was monitored by measuring the UV-visible spectrum of the solution on a spectrophotometer (T60 UV-vis spectrophotometer) operating at a resolution of 1 nm.

Characterization

The crystallinity and phases of the Ag nanoparticles were characterized by X-ray diffractometer (XRD-6000, Shimadzu, Japan) with Cukα radiation (λ = 1.5412 Å) in the range of 30°–90° with 2°/min scanning rate. The functional groups of Ag nanoparticles were characterized by Fourier-Transform Infrared (FTIR, Perkin Elmer, Spectrum BX) spectroscopy in the range of 4000–350 cm^{-1}. In addition, time- resolved absorption spectra of prepared Ag nanoparticles was analyzed via UV-visible Spectrophotometer (T60 UV-Vis spectrophotometer). The morphology and size of the prepared Ag nanoparticles was observed by Transmission Electron Microscopy.

Evaluation of antibacterial activity

The antimicrobial screening of the silver nanoparticles was carried out against *Escherichia coli*, *Klebsiella pneumoniae*, *Bacillus subtilis*, *Staphylococcus aureus*, *Aspergillus niger*, *Rhizopus stolonifer* and *Candida albican* using Agar-well diffusion method.

Table 1. The variations in zone of inhibitions (mm).

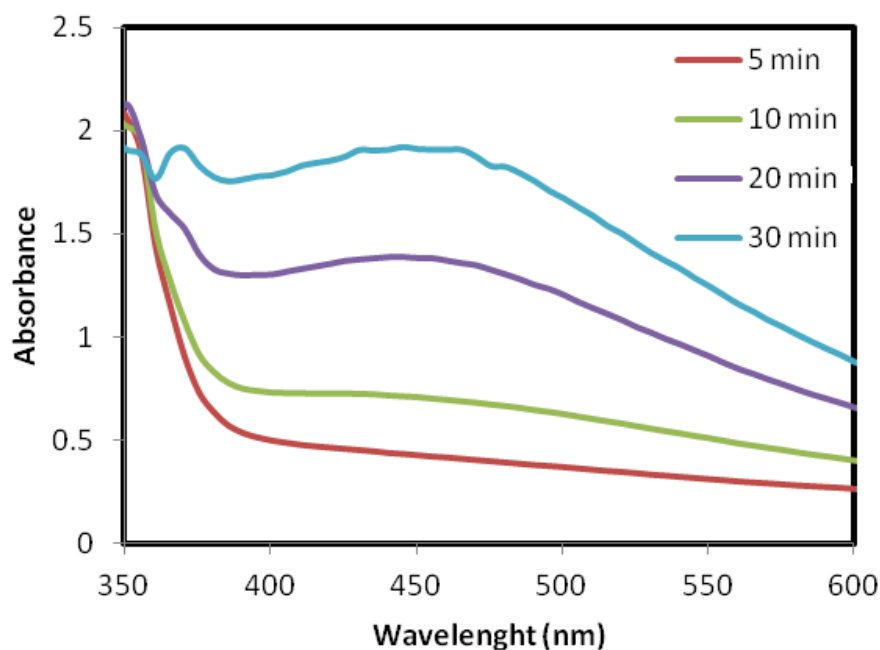| AgNp conc. (mg/ml)	Zone of inhibition of tested pathogenic bacteria (mm)				Zone of inhibition of tested pathogenic fungi (mm)		
	S. aureus	*E. coli*	*B. subtilis*	*K. pneumonia*	*A. niger*	*C. albican*	*R. stolonifer*
500	26	25	20	13	18	17	ND
250	24	21	19	11	15	14	ND
125	21	17	14	10	12	12	ND
62.5	18	14	13	ND	10	9	ND
31.25	12	10	10	ND	ND	ND	ND

ND=Not detected.

Figure 1. UV-visible spectrum of the silver nanoparticles synthesized with aqueous seed extract of *G. kola*

Gentamycin and Tioconazole were used as control for bacteria and fungi respectively. Using a micropipette, 50 µL of nanoparticle solution was poured onto each of the 8mm diameter well made on the prepared agar plates. On incubation at room temperature for 72 h, the diameter of zone inhibition was measured in millimeter; the values are shown in Table 1.

RESULTS AND DISCUSSION

UV- Vis spectra analysis

The color change was noted by visual observation in the Erlenmeyer flask that contains $AgNO_3$ solution with *G. kola* extract. The color of the $AgNO_3$/seed extract solution changed from light yellow to light brown after 5 min and eventually to dark brown. This color change indicates the formation of Ag nanoparticles in the solution. Seed extract without $AgNO_3$ did not show any color changes. The formation of Ag nanoparticles was further confirmed by using X-ray diffraction (XRD), Fourier-Transform infrared spectroscopy (FTIR) and Transmission electron microscopy (TEM).

Figure 1 shows the UV-vis absorption spectrum of the synthesized Ag nanoparticles. Silver nanoparticles have free electrons, which give surface plasmon resonance (SPR) absorption band. This is due to the combined vibration of electrons of silver nanoparticles in resonance with light wave. A broad absorption peak was observed at 440 nm, which is a characteristic band for silver nanoparticles. No other peak was observed in the spectrum which confirms that the synthesized products are Ag° only.
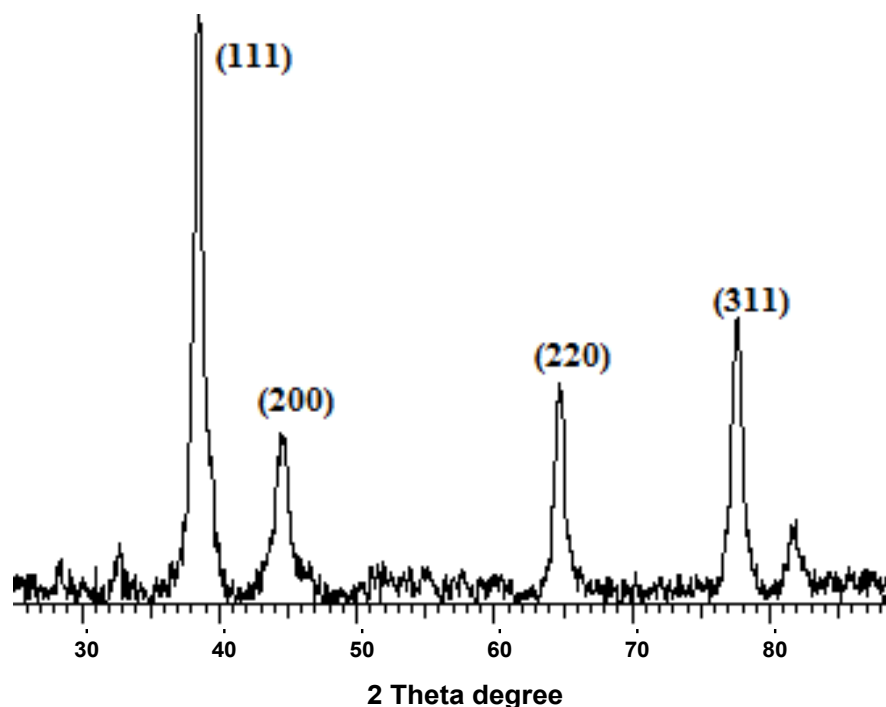
Figure 2. XRD patterns of Ag-NPs synthesized with *G. kola*.

XRD analysis

Figure 2 shows XRD patterns for Ag nanoparticles synthesized by *G. kola* seed extract. Four peaks at 2θ, 38.4, 44.5, 64.8, and 77.7 corresponding to (111), (200), (220) and (311) reflect planes of face-centred cubic (fcc) structure of Ag. These peaks are consistent with the standard data file JCPDS No 04–0783 JCPD. The broadening of X-ray peaks observed is primarily due to the small particle size. The mean size of silver nanoparticles was calculated using the Debye-Scherrer's equation (Sheny et al., 2011). The average mean size of AgNPs was 10.40 nm. No peaks from any other phase were observed showing that single phase Ag with cubic structure nanoparticles has been obtained directly.

FTIR spectra analysis

FTIR measurements were carried out on both the extract and the silver nanoparticles from *G. kola*. This was done to identify the biomolecules for reduction, and efficient stabilization of the metal nanoparticles synthesized by *G. kola* seed extract. The FTIR spectrum of silver nanoparticles is shown in Figure 3b. The presence of peaks at 3434, 2346, 2096, 1643 and 1028 cm^{-1} was observed for the crude extract of *G. kola* (Figure 3a), which indicates that the silver nanoparticles may be surrounded by hydroxyl group, because the peaks indicate –OH symmetric stretching and C–O bonds in aliphatic or carboxylic compounds (Ghosh et al., 2012). The band at 3434 cm^{-1} corresponds to O-H stretching H-bonded alcohols. The peak at 1643 cm^{-1} corresponds to C=O of ketone or aldehyde group and was shifted to lower frequency of 1635 cm^{-1} in the spectra of the silver nanoparticles from *G. kola*. The peak at 1028 cm^{-1} was assigned to the stretch of the C−O bond (Renquan et al., 2012). Therefore, the synthesized nanoparticles were surrounded by proteins and metabolites such as terpenoids, biflavonoids having functional groups of alcohols, ketones, aldehydes and carboxylic acids. This suggests that the biological molecules could possibly perform dual functions of formation and stabilization of silver nanoparticles in the aqueous medium (Mukherjee et al., 2001). This shows that the aqueous seed extract of *G. kola* is a very good and robust bioreductant for the synthesis of silver nanoparticles.

TEM and EDX analysis

The TEM image gives the morphology and size of the synthesized silver nanoparticles. A spherical nanoparticle which conforms with the SPR band in the UV- Vis spectrophotometer and to that of the XRD analysis was obtained with average particle size of 10.40 nm (Figure 4). Table 2 shows the EDX profile of the synthesized silver nanoparticle from *G. kola* extract. The selected area electron diffraction SAED pattern of *G. kola* silver nanoparticles was recorded at different scales. The
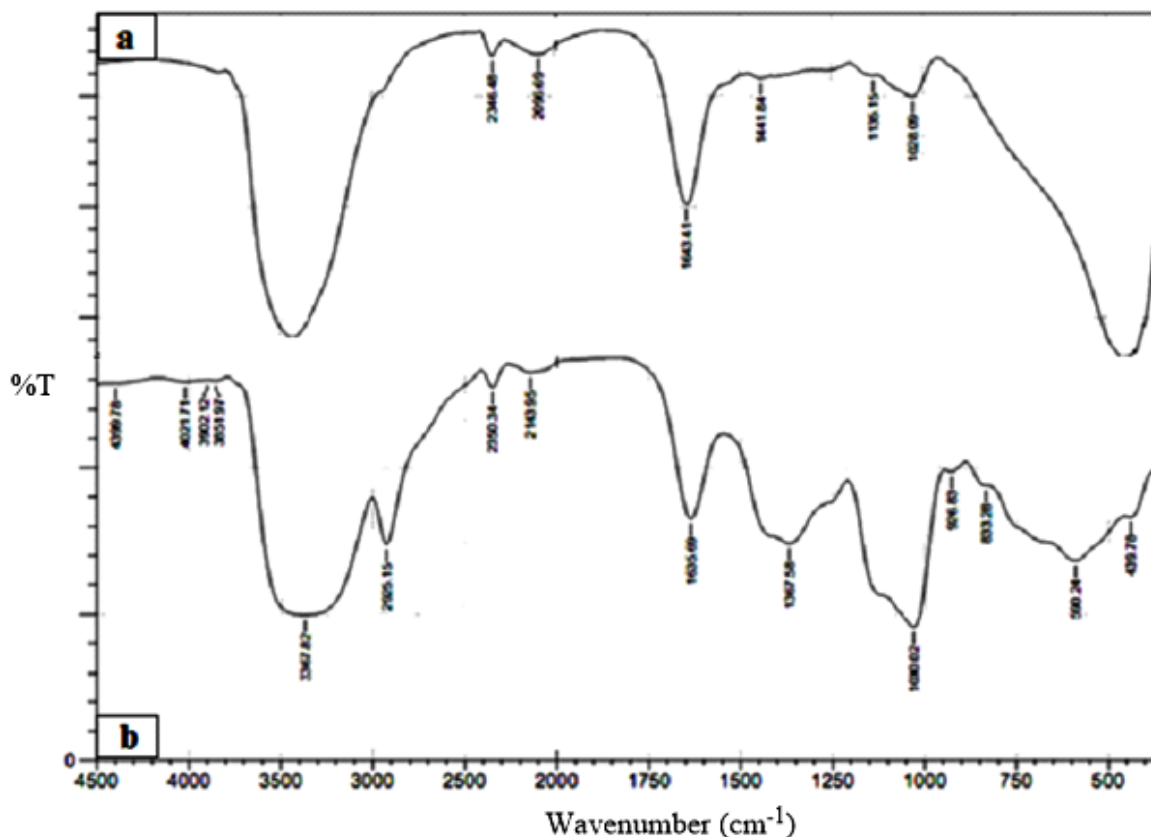
Figure 3. FTIR spectra of (a) extract of *G. kola* leave extract (b) silver nanoparticles synthesized using *G. kola*.

Table 2. EDX elemental analysis of the silver nanoparticles of *G. kola*.

Element sigma	Weight (%)	Weight %
C	57.23	0.57
O	16.94	0.20
Ag	25.82	0.73

observed spot resulting into a circular ring confirmed the polycrystalline nature and face centered cubic structure of GSNP. The circular spot corresponds to the (111), (200), (220) and (311) Plane of Ag°.

Antibacterial assay

The bio-reduced silver nanoparticles from *G. kola* show a clear and high zone of inhibition as a result of the attachment of the silver ion to the negative charged cell wall. This led to structural changes in the cell wall, permeabilility and subsequently death of the bacteria (Sondi and Salopek-Sondi, 2004) which prevent the multipilication of *Staphylococcus aureus*, *Escherichia coli*,

Klebsiella pneumoniae and *Bacillus subtilis;* likewise on fungal pathogen namely *Aspergillus niger* , *Rhizophus stolonifer* , and *Candida albican*. S. *aureus* shows the highest zone of inhibition at 500mg/L compared to Gentamycin while *K. pneumoniae* shows the lowest. For fungal pathogen, both A. *niger* and *Candida albican* show same efficacy compared to Tioconazole; *R. stolonifer* shows no zone of inhibition (Table 1).

Also due to high zone of inhibition exhibited by S. *aureus* and A. *niger* followed by *C. albican* in Figure 5, the silver nanoparticles from *Garcinia kola* possess high antimicrobial activity which can be used in household appliances like clothes washer and refrigerator which can kill bacteria and reduce odour

Conclusion

In this paper, we have reported a green method to synthesize silver nanoparticles using the aqueous seed extract of *G. kola*. The aqueous seed extract of *G. kola* helped in reducing and stabilizing the silver nanoparticles with remarkable growth onset of 10 min. This makes our green approach superior to conventional methods. The average size was found to be 10.4 nm with high
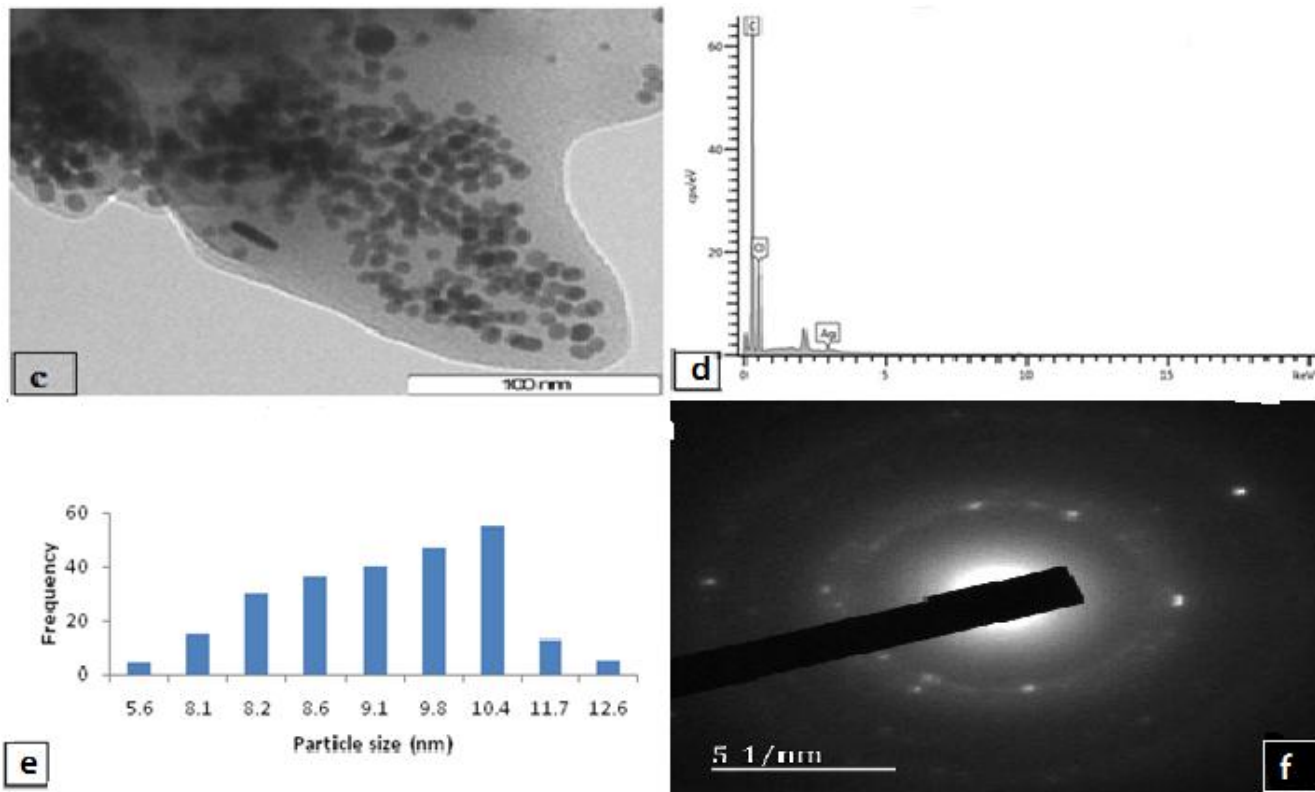
Figure 4. (c) TEM micrograph of the Ag nanoparticles synthesized using *G. kola* (d) EDX graph (e) the particle size distribution of the synthesized silver nanoparticles from *G. kola.* (f) selected area electron diffraction (SAED) pattern of the synthesized silver nanoparticles from *G. kola.*
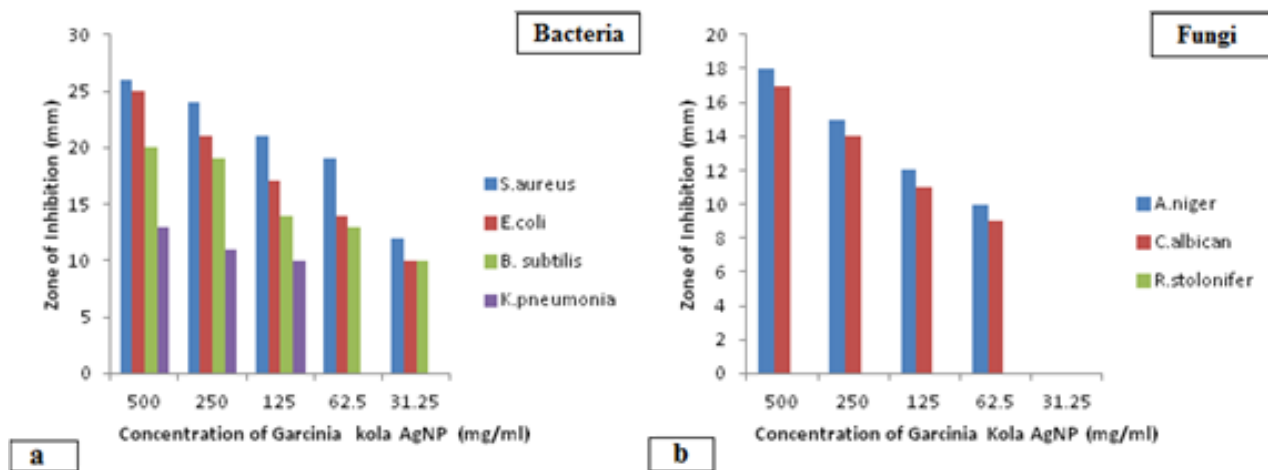
Figure 5. Antimicrobial activity of silver nanoparticles synthesized from *G. kola.*

susceptibility against tested pathogenic bacteria and fungi.

Conflict of interests

The authors have not declared any conflict of interest.

REFERENCES

Adesuyi AO, Elumm IK, Adaramola FB, Nwokocha AGM (2012). Nutritional and Phytochemical Screening of Garcinia kola. Adv. J. Food Sci. Technol. 4:9-14.

Ahmad A, Mukherjee P, Senapati S, Mandal D, Khan MI, Kumar R, Sastry M (2003). Extracellular biosynthesis of silver nanoparticles using the fungus *Fusarium oxysporum*. Colloids Surf. B Biointerfaces 28:313-318.

Anjali B, Haresh K, Deshpande MP (2013). Eco-friendly phyto-synthesis of silver nanoparticles using Jatropha seedcake extract. Chin. Phys. Lett. 30(12):128103.1-128103.5

Ashokkumar S, Ravi S, Kathiravan V, Velmurugan S (2015). Synthesis of silver nanoparticles using *A. indicum* leaf extract and their antibacterial activity. Spectrochim. Acta A Mol. Biomol. Spectrosc. 134:34-39.

Babak S, Gholamhoseinpoor F (2015). A study on the stability and green synthesis of silver nanoparticles using *Ziziphora tenuior* (Zt) extract at room temperature. Spectrochim. Acta A Mol. Biomol. Spectrosc. 134:310-315.

Balaji DS, Basavaraja S, Deshpande R, Bedre MD, Prabhakar BK, Venkataraman A (2009). Extracellular biosynthesis of functionalized silver nanoparticles by strains of *Cladosporium cladosporioides* fungus. Colloids Surf. B Biointerfaces 68:88-92.

Bulent U, Haluk T, Ahmet C, Ahmet M (2015). Role of irradiation in the green synthesis of silver nanoparticles mediated by fig (*Ficus carica*) leaf extract. Spectrochim. Acta A Mol. Biomol. Spectrosc. 135:153-161.

Chandrakant KT, Sreekantha RD, Rohini A, Sungha P, Atul K, Sushma S (2013). Green synthesis of silver nanoparticles and their application for the development of optical fiber based hydrogen peroxide sensor. Sens. Actuators B Chem. 183:144-149.

Chengcai L, Yuhong Z, Xiaowei Z, Yuewu Z, Yanguang W (2005). The role of poly(ethylene glycol) in the formation of silver nanoparticles. J. Colloid. Interface Sci. 288:444-448.

Dare EO, Oseghale CO, Labulo AH, Adesuji ET, Elemike EE, Onwuka JC, Bamgbose JT (2015). Green synthesis and growth kinetics of nanosilver under bio-diversified plant extracts influence. J. Nanostruct. Chem. 5:85-94.

Deenadayalan AK, Palanichamy V, Selvaraj MR (2014). Green synthesis of silver nanoparticles using *Alternanthera dentata* leaf extract at room temperature and their antimicrobial activity, Spectrochim. Acta Part A Mol. Biomol. Spectrosc. 127:168-171.

Elemike EE, Oseghale OC, Aleruchi C, Labulo AH, Owoseni MC, Mfon R, Dare EO, Adesuji ET (2014). Evaluation of antibacterial activities of silver nanoparticle green-synthesized using pineapple leaf. Micron 57:1-5.

Ghosh S, Patil S, Ahire M, Kitture RK, Pardesi S, Swaranjit K, Bellare C, Dhavale J, Jabgunde A, Chopade B (2012). Synthesis of silver nanoparticles using Dioscorea bulbifera tuber extract and evaluation of its synergistic potential in combination with antimicrobial agents A. Int. J. Nanomed. 7:483-496.

Gnanasekar S, Chandrakasan G, Karuppiah K, Vedagiri H, Kumpati P, Sivaramakrishnan S (2012). Phyto-synthesis of silver nanoscale particles using Morinda citrifolia L. and its inhibitory activity against human pathogens. Colloids Surf. B Biointerfaces 95:235-240.

Gurunathan S, Kalishwaralal K, Vaidyanathan R, Deepak V, Pandian SRK, Muniyandi J (2009). Biosynthesis, purification and characterization of silver nanoparticles using *Escherichia coli*. Colloids Surf. B Biointerfaces 74:328-335.

He SY, Guo ZR, Zhang Y, Zhang S, Wang J, Gu N (2007). Biosynthesis of gold nanoparticles using the bacteria *Rhodo pseudomonas capsulate*. Mater. Lett. 61:3984-3987.

Hebeish A, El-Shafei A, Sharaf S, Zaghloul S (2011). Novel precursors for green synthesis and application of silver nanoparticles in the realm of cotton finishing. Carbohydr. Polym. 84:605-613.

Hoskote AKK, Badal KM, Kesarla MK, Sireesh BM, Tammina SK, Pavithra M, Asit RG (2014). Antimicrobial and antioxidant activities of Mimusops elengi seed extract mediated isotropic silver nanoparticles. Spectrochim. Acta A Mol. Biomol. Spectrosc. 130:13-18.

Ibikunle GF, Emmanuel OO (2011). Evaluation of Garcinia Kola Nuts For Antitrichomonal Activity. J. Pharm. Biol. Sci. 2:264-269.

Jain D, Daima HK, Kachhwaha S, Kothari SL (2009). Synthesis of plant-mediated silver nanoparticles using papaya fruit extract and evaluation of their anti microbial activities. Dig. J. Nanomater. Biostruct. 4:723-726.

Judita P, Dovile J, Irena M, Joana S, Ina J, Rokas K (2014). Biosynthesis of silver nanoparticles using lingonberry and cranberry juices and their antimicrobial activity. Colloids Surf. B Biointerfaces 121:214-221.

Korbekandi H, Iravani S, Abbasi S (2012). Optimization of biological synthesis of silver nanoparticles using *Lactobacillus casei*. J. Chem. Technol. Biotechnol. 87:932-937.

LÜ F, Gao Y, Huang J, Sun D, Li Q (2014). Roles of Biomolecules in the Biosynthesis of Silver Nanoparticles: Case of *Gardenia jasminoides* extract. Chin. J. Chem. Eng. 22(6):706-712.

Lu Y, Yin Y, Mayers BT, Xia Y (2002). Modifying the surface properties of superparamagnetic iron oxide nanoparticles through a sol-gel approach. Nano Lett. 2(3):183-186.

Mariselvama R, Ranjitsingh AJA, Usha RNA, Kalirajan K, Padmalatha C, Mosae SP (2014). Green synthesis of silver nanoparticles from the extract of the inflorescence of *Cocos nucifera* (Family: Arecaceae) for enhanced antibacterial activity. Spectrochim. Acta A Mol. Biomol. Spectrosc. 129:537-541.

Mukherjee P, Ahmad A, Mandal D, Senapati S, Sainkar SR, Khan MI, Ramani R, Parischa R, Ajaykumar PV, Alam M, Sastry M, Kumar R (2001). Bioreduction of $AuCl_4^-$ Ions by the fungus, *Verticillium* sp. and surface trapping of the gold nanoparticles formed. Angew. Chem. Int. Ed. 40:3585-3588.

Narendra S, Khanna PK (2007). *In situ* synthesis of silver nano-particles in polymethylmethacrylate. Mater. Chem. Phys. 104:367-372.

Oxana V, Kharissova HV, Rasika D, Boris IK, Betsabee OP, Victor M, Jimenez P (2013). The greener synthesis of nanoparticles. Trends Biotechnol. 31(4):240-248.

Pradnya N, Poulomi M, Sudhir K (2014). Biosynthesis characterization and antibacterial studies of silver nanoparticles using pods extract of Acacia auriculiformis. Spectrochim. Acta A Mol. Biomol. Spectrosc. 129:121-124.

Renquan L, Yang D, Cui D, Wang Z, Guo L (2012). Egg white-mediated green synthesis of silver nanoparticles with excellent biocompatibility and enhanced radiation effects on cancer cells. Int. J. Nanomedicine 7:2101-2107.

Sheny DS, Mathew J, Philip D (2011). Phytosynthesis of Au, Ag and Au-Ag bimetallic nanoparticles using aqueous extract and dried leaf of *Anacardium occidentale*. Spectrochim. Acta A Mol. Biomol. Spectrosc. 79:254-262.

Shinde NM, Lokhande AC, Lokhande CD (2014). A green synthesis method for large area silver thin film containing nanoparticles. J. Photochem. Photobiol. B 136:19-25.

Sondi I, Salopek-Sondi B (2004). Silver nanoparticles as antimicrobial agent: a case study on E. coli as a model for Gram-negative bacteria. J. Colloid. Int. Sci. 275:177-182.

Sun Y, Xia Y (2002). Shape-controlled synthesis of gold and silver nanoparticles. Science 298(5601):2176-2179.

Tien DC, Liao CY, Huang JC, Tseng KH, Lung JK, Tsung TT, Kao WS, Tsai TH, Cheng TW, Yu BS, Lin HM, Stobinski, L (2008). Novel technique for preparing a nano-silver water suspension by arc-discharge method. Rev. Adv. Mater. Sci. 18:750-756.

Tsuji T, Kakita T, Tsuji M (2003). Preparation of nano-size particle of silver with femtosecond laser ablation in water. Appl. Surf. Sci. 206:314-320.

Venkata SK, Susmila AG, Subba RY, Prasad TNVKV, Varada RA, Sai Gopa DVR (2014). Biofabrication of silver nanoparticles using Andrographis paniculata, Eur. J. Med. Chem. 73:135-140.

Yang H, Song X, Zhang X, Ao W, Qiu G (2003). Synthesis of vanadium-doped SnO_2 nanoparticles by chemical co-precipitation method". Mater. Lett. 57(20):3124-3127.

Yong Z, Yu SH, Wang CY, Li XG, Zhu YR, Chen ZY (1999). A Novel Ultraviolet Irradiation Photoreduction Technique for the Preparation of Single-Crystal Ag Nanorods and Ag Dendrites. Adv. Mater. 11(10):850-852.

Full Length Research Paper

Assessment of anti-corrosion potentials of extract of *Ficus asperifolia* -Miq (Moraceae) on mild steel in acidic medium

Fadare, O. O.[1]*, Okoronkwo, A. E.[2] and Olasehinde, E. F.[2]

[1]Department of Pharmacognosy, Obafemi Awolowo University, Ile-Ife, Osun State, Nigeria.
[2]Department of Chemistry, Federal University of Technology, Akure, Ondo State, Nigeria.

The inhibitory potentials of ethanolic extracts and four fractions of the stem bark of *Ficus asperifolia* – Miq. for the corrosion of mild steel were assessed using weight loss method, Fourier atomic absorption spectroscopy, scanning electron microscopy (SEM). The effects of varying immersion period, concentration of the inhibitors and temperatures for mild steel corrosion in 5 M HCl acid solution were carried out. A detailed kinetic reaction, thermodynamic (Ea, ΔH, ΔS) and adsorption isotherm studies were obtained. The crude extract of *F. asperifolia* (EFA) has the highest inhibition efficiency of 55%. The inhibitory efficiency of the four fractions of *F. asperifolia* (EFA) compared with the crude extract was in the order ethyl acetate > n-hexane > butanol > EFA > Aqueous. The inhibition efficiency was found to increase with increase in the extracts concentration but decreased with temperature. Corrosion rate increases with time but decreases with extracts concentration. The kinetic studies of the data followed a first order reaction. Thermodynamic studies revealed that corrosion inhibition may be due to spontaneous mixed adsorption of the plant constituents on the metal surface. Experimental data were fitted to Langmuir, Freundlich and Temkin adsorption isotherms. The plant investigated showed a good potential for green corrosion inhibitors. Investigation of phytochemical constituents showed that the extracts contain alkaloids, flavonoids, saponins, tannins anthraquinones and reducing sugars.

Key words: Inhibitory efficiency, corrosion rate, adsorption isotherm.

INTRODUCTION

Mild steel has found urge and umpteen importance in the developing countries, emerging economies as well as developed world as it forms the backbone of industrialization. One of the most challenging and difficult tasks for industries are the protection of metals from corrosion (Al-Otaibi et al., 2012). Acidic solutions are widely used in industries and the areas of application are acid pickling, industrial acid cleaning, acid descaling and oil-well cleaning (Schmitt, 1984; Ashassi-Sorkhabi et al., 2009). Corrosion inhibitors are needed to reduce the corrosion rates of metallic materials in these acidic media (Lagrenee et al, 2002). Phyto-inhibitors now attract more attention in the research world over the synthetic counterparts due to their low level or no toxicity, eco-

friendliness, availability, affordability and efficient nature of this class of inhibitors (Al-Otaibi et al., 2012). The synthetic inhibitors are now generating greater environmental concerns due to toxic effect of the synthetic compounds on human and animal life during their production and use.

Ficus asperifolia (Moraceae) is a small or average size tree, terrestrial or epiphyte which can reach 20 m in height (Adjanohoun et al., 1996; Omoniwa and Luka, 2012). *F. asperifolia* inhabits tropical rainforests in Senegal, Uganda, Tanzania, Natal (South Africa), Madagascar and Cameroon. It is also found across many states in Nigeria (Omoniwa and Luka, 2012). Common/local names of *F. asperifolia* include Sand paper leaf (English); *Epin* (Yoruba); *Ebameme* (Benin); *Fula-pulaar* (Guinea); *Safen* (Senegal) and *Manding-mandinka* (Sierra Leone). *Ficus asperifolia* is used as analgesic, anti-tumors, anti-cancer, diuretic, abortificients, ecbolics and menstrual cycle pain reliever as well for treating nasopharyngeal infections, oedema, gout and veneral diseases (Adjanohoun et al., 1996). However, the stem bark of F. asperifolia has not been investigated for its corrosion inhibition.

The successful use of phytoconstituents as corrosion inhibitors in acidic media have been reported by some researchers (Olasehinde et al., 2013, Olusegun et al., 2013, Fouda et al., 2014, Ismail et al., 2011, Devarayan et al., 2012, Abdulrahmanet al., 2011, Ten et al., 2012, Chen et al., 2013, Behpour and Mohammadi, 2012; Negm et al., 2012). Efforts were made in this study to establish the inhibitory efficiency of *F. asperifolia* (Miq- Moraceace) stem bark extracts and the respective fractions; towards activity-directed purification of the plant extracts for better or improved inhibitory activities.

EXPERIMENTAL

Materials preparation

Mild steel of known elemental composition (%) was used for this study: Mn (0.56), S (0.03), P (0.02), C (0.12), Si (0.17), Cu (0.28) and the rest Fe. It was mechanically pressed cut into coupons of dimensions 18 × 16 × 4 mm before carrying out corrosion test on them. The coupons were used as supplied without any form of polishing but surface treatment of the coupons by degreasing in absolute ethanol and drying in acetone were carried out. The coupons were then preserved under air tight dessicator with activated dessicant to avoid contamination before their use in the corrosion studies (Eddy and Ebenso, 2008; James and Akaranta, 2009). All the solvents used for this study were redistilled before usage to ensure purity.

Collection, authentication, preparation and extraction of plant materials

The stem bark of the plant, *F. asperifolia* was collected in June, 2014 at Ile-Ife, Nigeria. The plant material was authenticated at the Botany Department, Obafemi Awolowo University, Ile-Ife. The stem bark was cut into pieces, washed thoroughly with water, and dried using vacuum drying oven at 40°C. The sample was pulverized using *Buchi* milling machine (1200 rpm) and stored for

further analysis.

Powdered stem bark of *F. asperifolia* was soaked in 80% ethanol for 72 h. It was filtered and extract was concentrated in-vacuo to dryness using rotary evaporator and the weight of the extract was determined. Five different concentrations (0.1, 0.2, 0.3, 0.4 and 0.5 g/100 mL) of the extract were prepared with 5 M hydrochloric acid solution and were used for all the experiments.

Chemical analysis

Qualitative and quantitative analysis of the crude extracts of *F. asperifolia* was carried out according to the method reported by Onyeka and Nwabekwe (2007).

Solvent partitioning: modified Kupchan partitioning method

The ethanolic extract (40.0 g) of *F. asperifolia* was suspended with 200 mL distilled water each, and successively partitioned into n-Hexane (1500 ml), ethylacetate (2800 ml), and n-Butanol (400 ml) based on the polarity of the extracts, and were in turn concentrated *in vacuo* to dryness to give four partitioned fractions (Wagenen et al., 1993). Five different concentrations (0.1, 0.2, 0.3, 0.4 and 0.5 g/100 ml) of each of the fractions were prepared with 5 M hydrochloric acid solution and were tested for corrosion inhibitory activities.

Gravimetric study

In the gravimetric study, a known weight metal (mild steel) coupon was completely immersed in 100 mL of the test solutions, the respective concentration of the blank (5 M HCl) and the inhibitor solutions for 4 h after which it was retrieved, washed with distilled water, alcohol, dried and weighed. The difference in weight for a period of 4 h was taken as weight loss.

From the weight loss results, corrosion rate (CR) and percentage inhibition efficiency (I.E%) were calculated using Equations 1 and 2.

$$CR(gh^{-1}cm^{-1}) = \frac{\Delta W}{AT} \tag{1}$$

where ΔW is weight loss, that is, $W_i - W_f$, A is the area of the mild steel coupon (in cm^2) and T is immersion time (in hours)

$$I.E\% = (1 - CR_{inh}/CR_{Blank}) \times 100 \tag{2}$$

where CR_{inh} and CR_{Blank} correspond to the corrosion rates in the presence and absence of inhibitor respectively.

The surface coverage was calculated by using Equation 3:

$$\theta = (1 - CR_{inh}/CR_{Blank}) \tag{3}$$

Kinetic studies

In order to investigate the order of the reactions and evaluate the mass loss, the experiments were carried out at room temperature at various inhibitor concentrations of 0.1 to 0.5 g/100 mL extract in 5 M HCl. The pre-weighed coupons were immersed in 100 mL of the respective inhibitor/blank solutions. The coupons were retrieved from the solutions, washed in distilled water, alcohol, dried and weighed at 24 h interval progressively for 7 days. The order of

reaction and half life were determined from the results obtained using Equations 4 and 5 respectively.

$$\ln(W_1 - W_2) = -kt + \ln W_1 \qquad (4)$$

where W_1 is the initial weight of the metal, W_2 is the final weight, t is the duration of immersion (time) or exposure of the metal to acidic medium, and k is the rate constant.

From the rate constant k, the half life ($t_{1/2}$) can be calculated using:

$$t_{1/2} = 0.693/k \qquad (5)$$

Temperature variation

The pre weighed coupons were dipped in 100 mL of the various concentrations of the inhibitors/blank solution ranging from 0.1 to 0.5 g/100 mL in 5 M HCl and maintained at 303, 313, 323 and 333k in a thermostatic water bath for 4 h. This was replicated. After which it was retrieved, rinsed in distilled water, degreased in ethanol, dried in acetone and weighed. The results obtained were fitted into different isotherms and the thermodynamic parameters were calculated.

Atomic absorption spectroscopy (AAS) analysis

Atomic absorption analysis was conducted by using atomic absorption spectrometer model PerkinElmer AAnalyst 400. This was carried out to determine the concentration of iron (II) ions in 5 M HCl after 4 h immersion time in the presence of the extracts of *F. asperiofolia*. The pre-weighed coupon was immersed in a solution of HCl containing the plant extract for 4 h to examine the amount of Iron (II) in the acidic solution.

The calibration curve of iron (II) ions was drawn before analyzing the electrolyte solution. All samples containing iron (II) were diluted with distilled water to ensure that the concentration of metal ions is within the range of the calibration curve.

Scanning electron microscopy (SEM) analysis

The surface morphological analysis of mild steel after 4 h immersion in 5M HCl containing 1% $^W/_v$ EFA extract was studied to understand the changes that occur during the corrosion of mild steel in the presence and absence of stem bark extracts using scanning electron microscope (Model: Aspex 3020).

RESULTS AND DISCUSSION

Phytochemical constituents of F. asperifolia

Corrosion inhibition performance of organic compounds can be evaluated using electrochemical and chemical techniques (Obi-Egbedi and Obot, 2010). Presence of secondary metabolites in plants extracts has been identified to be responsible for the corrosion inhibitory properties on metal surface (Vijayalakshmi et al., 2011; Ating et al., 2010, Okafor et al., 2012)

Phytochemical screening of *F. asperifolia* using

qualitative methods revealed the presence of Alkaloids, saponnin, tannins, anthraquinones, cardiac glycosides and flavonoids while the quantitative phytochemical analysis revealed that flavonoid, saponin, tannin, cardiac glycoside and terpenoid has 52., 72.4, 31.2, 11.5 and 29.8 mg/ml respectively (Table 1). The chemical structures of most of these phyto-constituents contained electron rich bond or hetero atoms that facilitate their electron donating ability; hence the inhibition of the corrosion of mild steel by ethanolic extracts of *F. asperifolia* is attributed to the phyto-constituents of the extract. Similar inferences have been reported by some researchers for the inhibition of the corrosion of mild steel by ethanol extract of some plants (Bendahou et al., 2006; Ebenso et al., 2008). Possession of π-electrons or suitable functional groups may facilitate the transfer of charge from the inhibitor's molecule to the charged metal surface (physical adsorption) or transfer of electron from the inhibitor's molecule to the vacant-orbital of the metal (chemical adsorption) (Eddy et al., 2011).

Ashassi-Sorkhabi et al. (2009) implicated tannins in their study as a corrosion inhibitor. The inhibitive properties of tannins have been attributed to the reaction of the polyphenolic fraction of the tannins moieties, which ensures effective protection of the metal surfaces (Loto, 1998; Anauda et al., 2005; Nnanna et al., 2010).

Flavonoids are widely distributed in plants and give the flowers and fruits of many plants their vibrant colours. Flavonoids have antioxidant activity, anti-allergic, anti-cancer, anti-inflammatory and anti-viral activities. Al-qudah (2011) established in his study, using three different types of flavonoids and about 92% inhibitory efficiency of these flavonoids was reported.

Terpenoids and other constituents also posses functional groups which are capable of chelating with metal ions and thus facilitate strong coordination on the metal surface (Oguzie, 2008).

Some of these phyto-constituents observed in the plant of study have been implicated in one corrosion inhibitory activity or the other. It was reported (Schmitt, 1984) that as a rule of thumb, N-containing compounds such as amines, amino acids and quaternary ammonium salts exert their best efficiencies in prevention corrosion of iron and steel in HCl solutions while they are relatively ineffective in H_2SO_4 and this behaviour is in good agreement with the obtained results in this study. An acceleration behavior was reported for mild steel in H_2SO_4 in the presence of some phenols and this behavior tends to decrease with the increase in the inhibitor concentration, while they behave very well as corrosion inhibitors in HCl solutions (Rengamani et al., 1994). These observations are similar to that obtained in this study.

Effect of time on weight loss

For the chemical methods, a weight loss measurement is

Table 1. Phytochemical screening of the stem bark of extracts of *F. asperifolia.*

Phytochemical test	*F. asperifolia*	
	Qualitative analysis	Quantitative analysis
Flavoniods	++	52.4±0.12
Saponnins	++	72.4±0.28
Tannins	++	31.2±0.10
Cardaic glycosides	+	11.5±0.12
Terpenoids	++	29.8± 0.11
Anthraquinones	+	N.D
Steroids	-	N.D
Alkaloids	+	N.D
Reducing Sugar	+	N.D

++ = Strong positive; + = positive - = negative; ND = not determined; Values are means ± SD for three determinations.
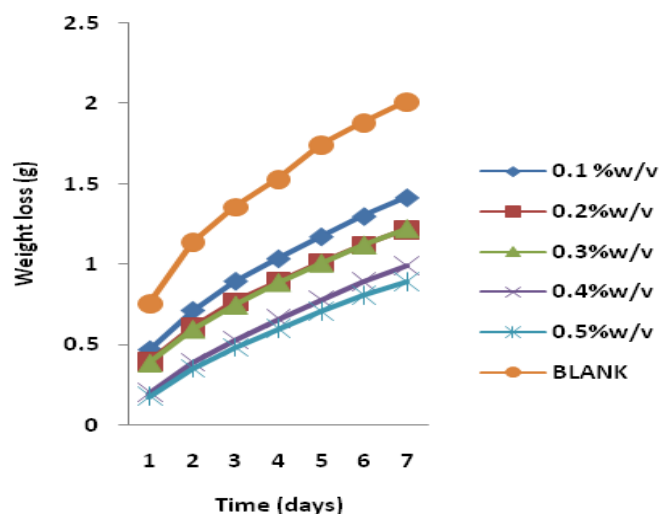

Figure 1. Variation of weight loss with respect to time for corrosion of mild steel in 5M HCl in the absence (Blank) and presence of crude extract of *F. asperifolia (EFA).*

ideally suited for long term immersion test. Corroborative results between weight loss and other techniques have been reported (Shukla and Quraishi, 2009; Singh and Quraishi, 2010; Obi-Egbedi and Obot, 2010). De Sauza and Spinelli (2009) reported that weight loss provides more reliable results than electrochemical techniques for the determination of corrosion rates and inhibition efficiency. Weight loss method is widely used for inhibition efficiency test (Obi-Egbedi and Obot, 2010; Musa et al., 2010; Khadom et al., 2010; Bouklahet al., 2006; Mercer, 1985). The simplicity and reliability of the measurement offered by the weight loss method are such that the technique forms the baseline method of measurement in many corrosion monitoring programmes (Obi-Egbedi and Obot, 2010; Afidah and Kassim, 2008).

Figure 1 shows the variation in weight-loss of mild steel

in 5 M HCl medium in the absence and presence of different concentration of the *F. asperifolia* stem bark extract as a function of time. The concentration of the extract varied from 0.1 to 0.5%$^w/_v$, and the time of immersion was varied from 0-168 hours at room temperature. From the results obtained, it was observed that weight-loss increase (up to 2.015 g) with increase in immersion time but decrease with increase in concentration of the extract to as low as 0.896 g at 0.5%$^w/_v$ EFA concentration.

The decrease observed in the weight loss with increase in the concentration of the extracts suggest an increased surface coverage on the metal and the adsorption of the phyto-constituents on the metal surface creating a barrier between the metal and the acidic medium. This enhances the inhibition of the metal from corroding due to the acidic environment hence reduction in weight loss with respect to the metal in the blank solution.

The plot of weight loss against time for the corrosion inhibition of mild steel in the presence and absence of the four fractions of the extract of *F. asperifolia* (EFA) namely: n-hexane, ethyl acetate, butanol and aqueous are shown in Figures 2 to 5.

From the plots, the weight loss increased with increase in immersion time but decreased with inhibitor concentration. The four fractions of *F. asperifoila* (EFA) followed similar trend with the crude extract but some of the fractions showed a greater inhibitory efficiency against corrosion compared to the crude extract.

Figures 6 and 7 compared the weight loss as well as the inhibitory efficiency within the four fractions and the crude extract of *F. asperifoila* (EFA). The result revealed that ethyl acetate fraction has the highest inhibitory efficiency amidst the four fractions and also better than the crude extract. This was followed by n-hexane, butanol, EFA and aqueous respectively. This suggests an increase in surface coverage by the phyto-constituents of the extract and the phyto-protective activity of the extract (Obi-Egbedi
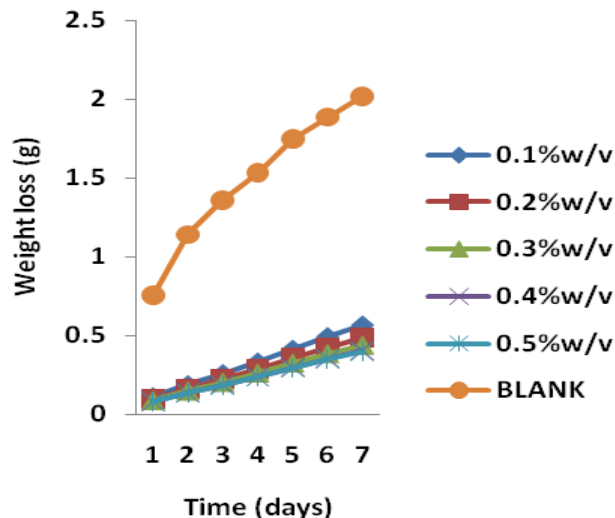
Figure 2. Variation of weight loss with respect to time for corrosion of mild steel in 5 M HCl in the absence (blank) and presence of n-hexane fraction of the extract of F. asperifolia (nEFA).
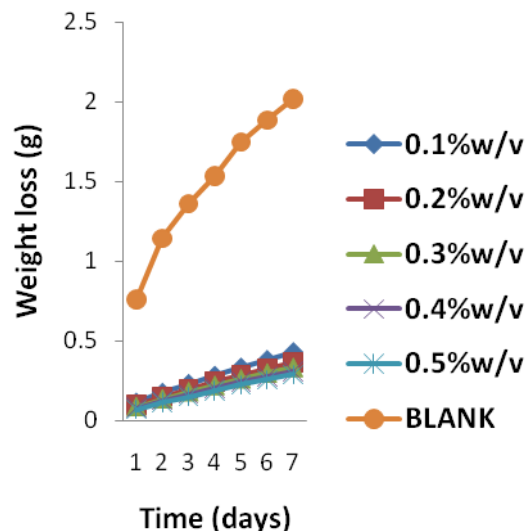

Figure 4. Variation of weight loss with respect to time for corrosion of mild steel in 5M HCl in the absence and presence of butanol fraction of the extract of *F. asperifolia* (bEFA).
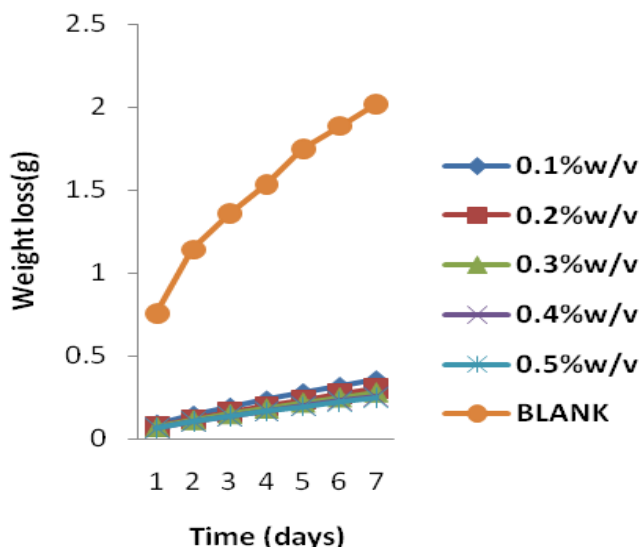

Figure 3. Variation of weight loss with respect to time for corrosion of mild steel in 5M HCl in the absence and presence of ethyl acetate fraction of the extract of F. asperifolia (eEFA).
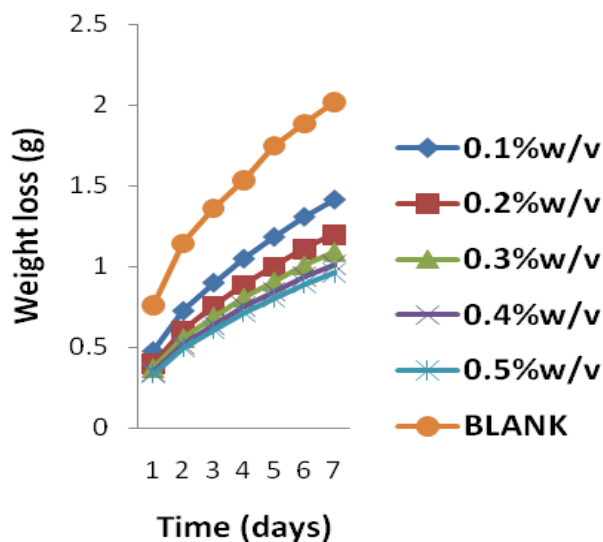

Figure 5. Variation of weight loss with respect to time for corrosion of mild steel in 5M HCl in the absence and presence of aqueous fraction of the extract of *F. asperifolia* (aEFA).

and Obot, 2010). It was also observed that further purification of the crude extract suggest better and greater inhibitory efficiency as well as reduction in the amount of inhibitor required per time for corrosion control.

Effect of extract concentration on inhibition efficiency

The effect of *F. asperifolia* extract concentrations on   the

dissolution of Iron (II) into acidic solution of 5 M hydrochloric acid for 4 h and the weight loss in each concentration of each extract were determined to assess the percentage inhibition efficiency of the extract. Figures 7 and 8 show the percentage inhibitory efficiency of *F. asperifolia* with varying extract concentration from 0.1 to $0.5\%^{w}/_{v}$ of the crude extract in 5 M hydrochloric acid and the concentration of Iron (II) in solution with   increase   in
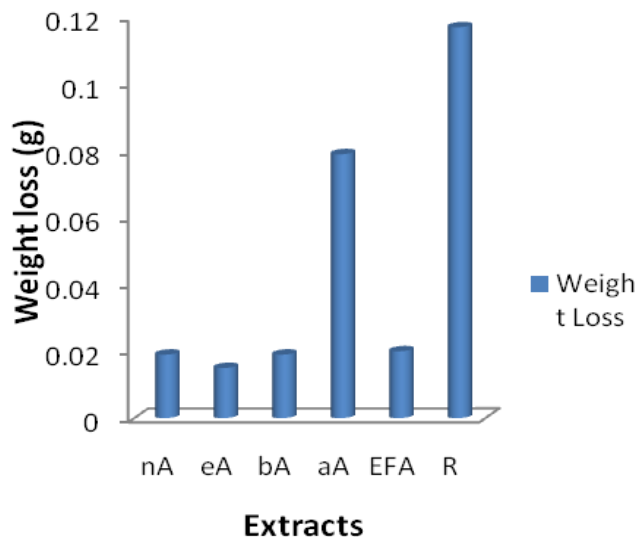
Figure 6. Comparison of weight loss within the fractions as well as the crude extract of *F. asperifolia.* nA, n-hexane; eA, ethyl acetate; bA, butanol; aA, aqueous; EFA, crude extract; R, Blank.

Figure 8. Variations in the concentrations of Fe^{2+} in 5M hydrochloric acid in the presence of *F. asperifolia.*
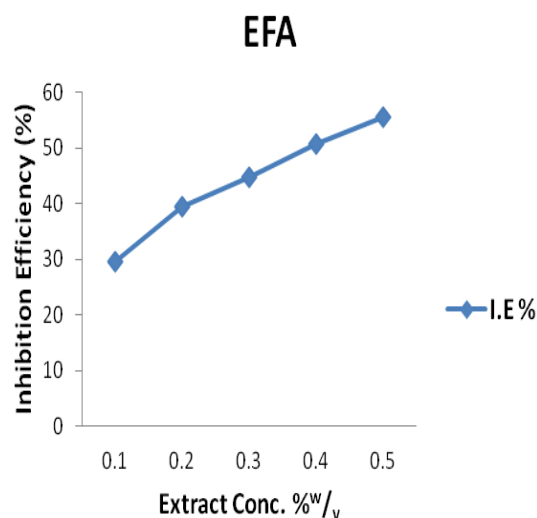

Figure 7. Inhibition Efficiency of different concentrations of EFA on mild steel in aqueous solution of 5M HCl for 4 h at room temperature.

the concentrations of the extract. There was an increase in the percentage Inhibitory efficiency of *F. asperifolia* from 29.6 to 55.5%. This is in agreement with other studies (James and Akaranta, 2009; Olasehinde et al., 2013; Owate et al., 2014). These results show that the plant under study is good green inhibitor against corrosion of mild steel. There is reduction in the concentrations of Fe^{2+} in solution as the concentration of the extract is increased. The decrease observed in the concentration of Fe^{2+} in
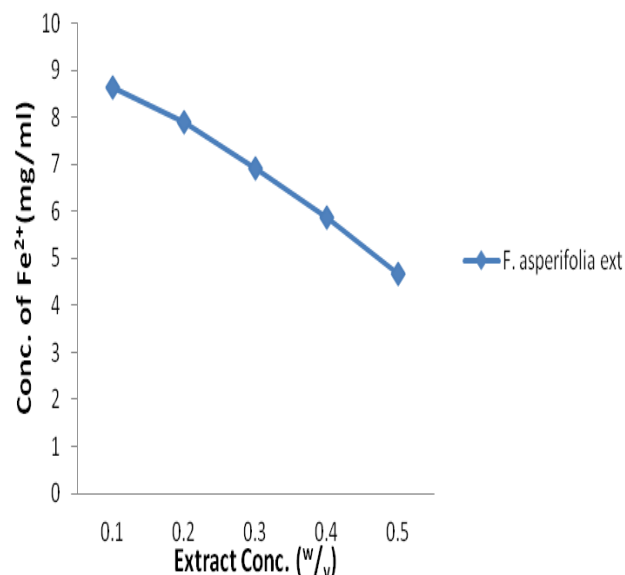
solution as the concentration of the extracts is being increased can be explained as the adsorption of the extract on the surface of the iron filing in acidic media which resulted in the resistance of the Fe ion against rapid oxidation of Fe^{2+}. Hence, reduction observed in the Fe^{2+} concentration in solution. This also further supports the inhibition activities of the plant extract under study. Similar results have been reported earlier (Johnsirani et al., 2012).

Effect of temperature on corrosion rate

Corrosion rate is a function of weight loss. Temperature is an important parameter in studies on metal dissolution studies (de Sauza and Spinelli, 2009). The corrosion rate in acid solutions, for example, increases exponentially with temperature increase because the hydrogen evolution over potential decreases (Popova et al., 2003). To assess the effect of temperature on corrosion and corrosion inhibitive process, weight loss experiments were performed at 10 K intervals in the temperature range 303 to 333 K in uninhibited acid (5 M HCl) and in inhibited solutions containing different concentrations of EFA as presented in Figure 9 to evaluate the stability of adsorbed layer/film of inhibitor on mild steel surface (Olasehinde et al., 2013). Corrosion rate of mild steel increased with increase in temperature but decreases with increase in the concentration of the extracts (Figure 9). There are similar observation reported in the literatures (Umoru et al., 2006; Ating et al., 2010; Vijayalakshmi et al., 2011; Ismail et al., 2011; Okafor et al., 2012). The rate of corrosion of mild steel increases as a result of increase in
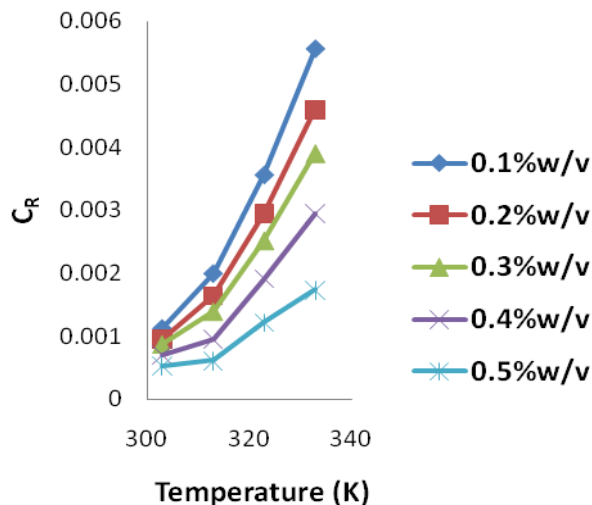
Figure 9. Variations of corrosion rate of mild steel with temperature in 5 M hydrochloric acid containing different concentrations of EFA.

Figure 11. A plot of In (W_1 - W_2) against time (days) for the adsorption of EFA on mild steel at room temperature.
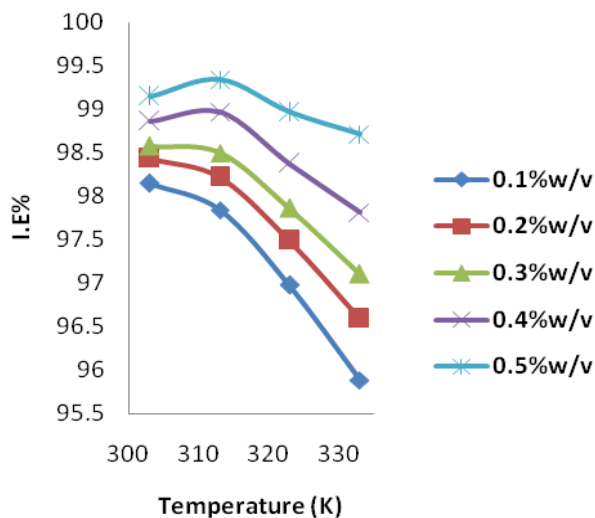

Figure 10. variations of corrosion rate of mild steel with temperature in 5 M hydrochloric acid containing different concentrations of EFA.

the average kinetic energy of the reacting molecules. However, the corrosion rate is much decreased for higher concentration of inhibited acid solution than the solution with low concentration of inhibitors. The decrease in the corrosion rate can be attributed to mitigating effect of the plant extract on the corrosion rate of the mild steel.

Effect of temperature on inhibition efficiency

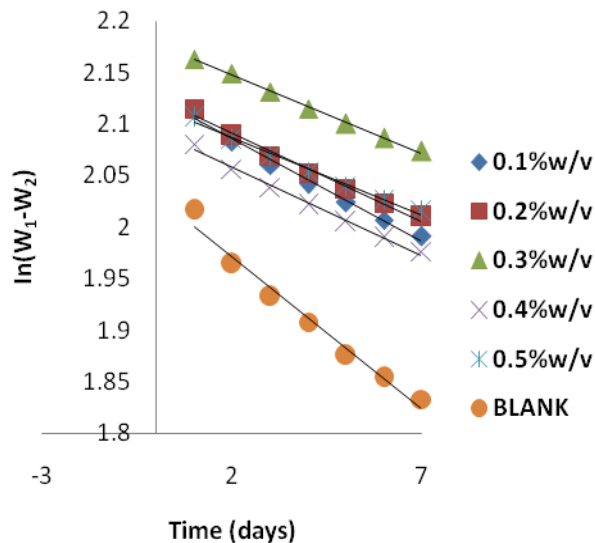To evaluate the stability of adsorbate on the   mild   steel

surface, weight loss measurements were carried out in the temperature range of 303 to 333 K in the presence and absence of extract of *F. asperifolia*. Corrosion rate has a corresponding relationship with inhibition efficiency and from the plot (Figure 10), it was observed that inhibition efficiency increase with increase in the concentration of the extract but decrease with increasing temperature due to increased rate of dissolution process of mild steel and partial desorption of the phyto-inhibitor from the mild steel surface with temperature. Therefore, decrease in inhibition efficiency with increase in temperature suggests a physisorptions mechanism of the inhibitor components onto the mild steel surface (Ating et al., 2010). This reveals the extracts under investigation as potent inhibitors for corrosion of mild steel in 5 M HCl (Olasehinde et al., 2013; Blaedel and Meloche, 1963).

Kinetic studies

In order to assess the stability of inhibitive behavior of the extracts on a time scale, weight loss measurement were performed in 5 M HCl acid solution in absence and presence of the extract EFA at 0.1 to 0.5%$^w/_v$ concentrations for 1 to 7 days at room temperature. The data obtained from the plots of variation of weight loss against time with respect to concentration were fitted into Equation (4) to test for the order of corrosion reaction in the presence of EFA. Representative plot for the first order reaction in different concentrations of the inhibitor is shown in Figure 11. The plots were linear with R^2 values of 0.9873, 0.9855, 0.9975, 0.9929 and 0.9906 at 0.1, 0.2, 0.3, 0.4 and 0.5% respectively. This indicates that a first order kinetic is applicable to the corrosion of mild steel   in

Table 2. The values of Rate Constant (K) and Half-life ($t_{1/2}$) for mild steel in 5M HCl in the absence and presence of different concentrations of EFA.

Conc. (%^{w}/$_v$)	Rate constant (K) of EFA	Half life ($t_{1/2}$) of EFA (days)
0.1	0.0198	35.0000
0.2	0.0170	40.7647
0.3	0.0152	45.5921
0.4	0.0151	45.8940
0.5	0.0150	46.2000
Blank	0.0296	23.4122

the presence of extracts of *F. asperifolia* as inhibitor. Also, the half lives ($t_{1/2}$) of the corrosion of mild steel in various media were calculated using Equation (5) (Nkuzinna et al., 2011). The values of rate constant (k) obtained from the slope of the plots of equation (4) and the values half life calculated from equation (5) is presented in Table 2.

From the results obtained the rate constant decreases with increase in the concentration of the extracts of EFA. Also, it is significant to note that half life increases with increase in concentration of the extract.

As the half-life increases, the corrosion rate decreases, which is an indication that more protection of the metals by the phyto-constituents of *F. asperifolia* extract. The findings were in accordance with James and Akaranta, 2009; Okaforet al., 2010; Olasehinde, 2013.

Scanning electron microscopy (SEM)

The surfaces of the mild steel strip used for the study were examined using scanning electron microscope model Aspex 3020 with 100X magnification. SEM micrographs of the mild steel before and after immersion in 5 M HCl solution in the absence and presence of inhibitors (EFA and EEC) are presented in Plates 1 to 3.

Surface analysis using scanning electron microscope provided more information on the level of attack as well as inhibition strength of the extract on the surface of the mild steel. The surface of the mild steel before immersion (Plate 1) appeared fine and smooth with a clear uniform pattern. This shows absence of any corrosion products formed on the metal surface (Johnsirani et al., 2012).

Plate 2 shows the micrograph of the mild steel immersed in 5M HCl solution in the absence of inhibitor for 4 h. The surface of the treated coupon shows etching composed of white and dark areas (Villamil et al., 1999; Fouda et al., 2014), the white areas represent the ferrite phase and the dark areas represent the pearlite (mixture of ferrite and cementite (FeC_3) in a lamellar form). It indicates clear disarrangement in the surface formation of the mild steel due to high metal dissolution rate and more active sites available for corrosion (Ji et al., 2012; Johnsirani et al., 2012).

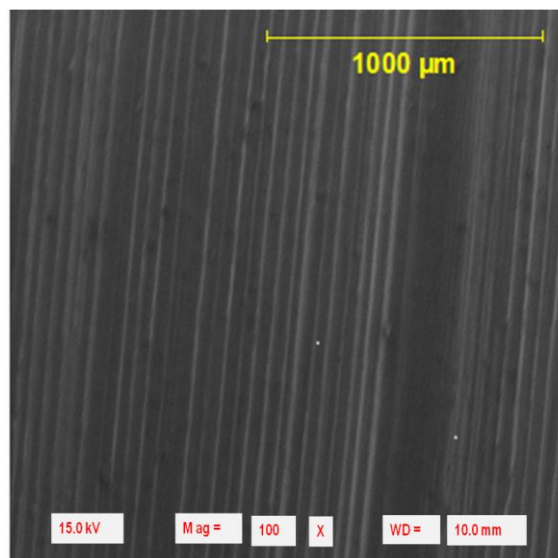The micrograph of the mild steels immersed in 5 M HCl

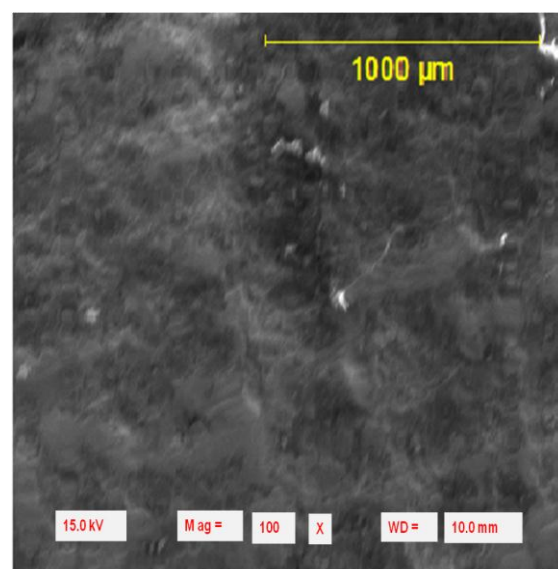**Plate 1.** SEM photograph of the mild steel prior to the corrosion study, that is, untreated mild steel sample.

Plate 2. SEM photograph of the mild steel treated with 5M HCl for 4 h without inhibitor.

Figure 12. Arrhenius plot for the mild steel in 5M HCl in different concentrations of EFA and the blank.
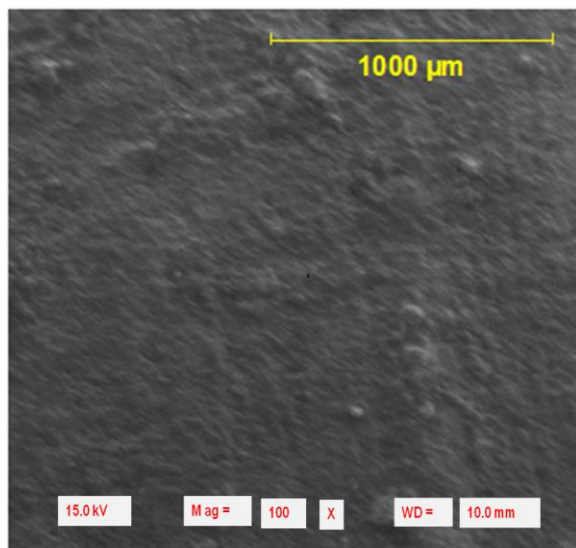
Plate 3. SEM photograph of the mild steel in 5M HCl for 4 h in the presence of 0.1%w/v of extract of *F. asperifolia* (EFA).

solution containing $0.1\%^w/_v$ EFA (Plate 3) shows that the surfaces were smoother when compared to the one without inhibitors. The plate shows less extensive attack in the presence of the extract than in the uninhibited acid. This implies that the extracts components adsorbed on the metal surface forming protective film over the surface of the mild steel thereby decreasing the mild steel dissolution in acidic medium. The protective film acts as a barrier between the steel and the acidic medium and thus retards the corrosion reactions (Loto et al., 2011). This is in line with various studies on plant extracts (Eddy and Ebenso, 2008; James and Akaranta, 2009; Dahmani et al., 2010; Sherine et al., 2010; Dauda et al., 2013; Nnanna et al., 2010; Fouda et al., 2014).

Thermodynamics studies

From Arrhenius equation (6), the logarithm of corrosion rate is a linear function of temperature. This was used to calculate the activation energy of the reactions in the presence and absence of the extract of EFA.

$$\log(C_R) = \log A - E_a/2.303RT \qquad (6)$$

Where C_R is the corrosion rate, E_a is the apparent activation energy, R is the molar gas constant, T is the absolute temperature and A is the Arrhenius pre-exponential factor. The Arrhenius plot obtained gave a straight line graph as shown in Figure 12 with a slope of $-E_a/2.303R$. The value of corrosion rate is jointly decided by the activation energy and the pre-exponential factor (Khadom et al., 2009).
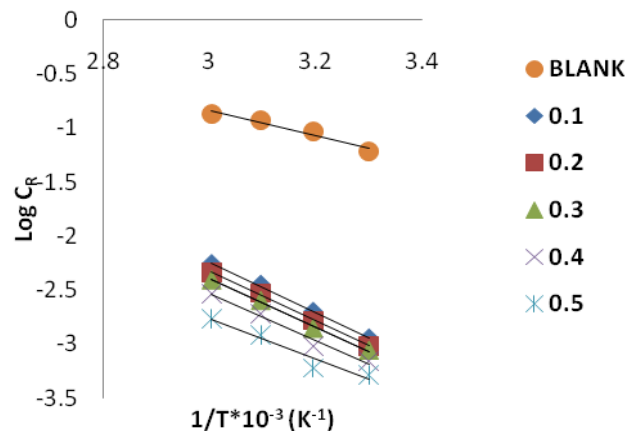
Analysis of the temperature dependence of inhibition efficiency as well as comparison of corrosion apparent activation energies in absence and presence of inhibitor gives some insight into the possible mechanism of inhibitor adsorption (Owate et al., 2014). A decrease in inhibition efficiency with the rise in temperature with analogous increase in corrosion activation energy in the presence of inhibitor compared to its absence is frequently interpreted as being suggestive of formation of an adsorption film of physical (electrostatic) nature. The reverse effect, corresponding to an increase in inhibition efficiency with rise in temperature and lower activation energy in the presence of inhibitor, suggests a chemisorptions mechanism (Popova et al., 2003; Ebenso, 2003; Oguzie et al., 2004).

Popova et al. (2003) gave the relationship between the temperature, percentage inhibition efficiency (I.E %) of an inhibitor and the activation energy in the presence of an inhibitor thus:

1. For an inhibitor whose I.E (%) decreases with temperature increase, the value of activation energy (E_a) found is greater than that in the uninhibited solution (blank solution).
2. For an inhibitor whose I.E (%) does not change with temperature variation, the value of activation energy (E_a) does not change in the presence or absence of inhibitors.
3. For an inhibitor whose I.E (%) increases with temperature increase, the value of activation energy (E_a) found is less than that in the uninhibited solution (blank solution).

While the higher value of the activation energy (E_a) of the process in an inhibitor's presence when compared to that in its absence is attributed to its physical adsorption, its chemisorptions is pronounced in the opposite case.

The values of activation energy obtained in this study as presented in Table 3, shows clearly that E_a values in   the

Table 3. Calculated values of activation parameters for mild steel corrosion in 5 M HCl in absence and presence of different concentrations of EFA extract.

Concentration (%^{w}/$_v$)	Activation Energy, Ea (kJmol^{-1})	Enthalpy of activation ΔH (kJmol^{-1})	Entropy of activation ΔS (kJmol^{-1})
0.1	45.0092	59.3561	-105.4089
0.2	44.4882	59.3561	-108.5778
0.3	42.8379	58.1690	-114.9997
0.4	42.1467	58.1690	-119.5778
0.5	35.9890	53.4205	-142.5467
Blank (5M HCl)	22.1226	27.8974	-147.2933

Table 4. Calculated parameters of three Adsorption Isotherms for Adsorption of the stem bark of *F. asperifolia* onto the mild steel surface.

Isotherm	Langmuir				Freundlich			Temkin	
Temp. (K)	Slope	R^2	(Kads)	ΔG	R^2	(1/n)	(K$_f$)	R^2	B (KJmol^{-1})
303	0.0242	0.9897	1.0214	-33.5739	0.9248	0.0059	0.0015	0.9240	9.8673
313	0.0375	0.9950	1.0262	-33.6130	0.9268	0.0091	0.0019	0.9257	9.9517
323	0.0487	0.9945	1.0366	-33.6971	0.9273	0.0119	0.0021	0.9256	9.8878
333	0.0688	0.9914	1.0509	-33.8108	0.9178	0.0169	0.0024	0.9153	9.8696

presence of different concentrations of the extract of EFA are higher than that of the uninhibited solution (blank solution). This increase in the presence of the extract of EFA denotes physical adsorption (Ebenso, 2003). This further buttress the increasing inhibition efficiency observed with increasing temperature for the adsorption of the extracts of EFA.

An alternative formulation of Arrhenius equation (Fouda et al., 2012) which is also referred to as Transition State (Equation 7):

$$C_R = [RT/nh] \, exp \, [\Delta S^*/R] \, exp \, [-\Delta H^*/RT] \qquad (7)$$

where C_R is the corrosion rate at absolute temperature T, R is universal gas constant, n is the Avogadro's constant, h is the Plank's constant, ΔS^* is the entropy of activation and ΔH^* is the enthalpy of activation.

Figure 14 shows a plot of Log (C_R/T) against 1/T, straight lines were obtained with a slope of (ΔH^o/2.303R) and an intercept of log $R/nh + \Delta S^*$/2.303R, from which the values of ΔS^* and ΔH^* were calculated. This is presented in Table 4.

From the Table, the activation energy (E$_a$) for *F. asperifolia* extract ranges from 35.989 to 45.009 kJmol^{-1}. The average activation energy value obtained for blank is 22.12 kJ/mol. This value is lower than that obtained for a system containing different concentrations of EFA. This

result suggests that EFA is adsorbed on the surface of mild steel by physical means (Popova et al., 2003; Awad, 2006).

The data showed that the positive values for ΔH enthalpy of activation both in the absence and presence of the extracts reflect the endothermic nature of the mild steel dissolution process (Khadom et al., 2010). It is evident that the activation enthalpies vary in the same trend as the activation energies. The value of enthalpy of activation (ΔH) for *F. asperifolia* extracts ranges from 53.4205 to 59.356 kJmol^{-1}.

The values of entropies of activation (ΔS) for *F. asperifolia* extract range from -105.408 to -142.546 kJmol^{-1} implies that the activated complex in the rate determining step represents association rather than dissociation, meaning that there is a reduction in disorderliness on going from reactant to activated complex. Similar observations were made by Oguzie (2008), Tao et al. (2009), Fouda et al. (2009), Obi-Egbedi and Obot (2012) and Ansari et al. (2014).

The standard free energy of adsorption, ΔG^o_{ads}, which can characterize the interaction of adsorption molecules and metal surface, was calculated using Equation 8

$$K_{ads} - 1/55.5 \, exp[\Delta G^*ads/RT] \qquad (8)$$

This can also be expressed as:

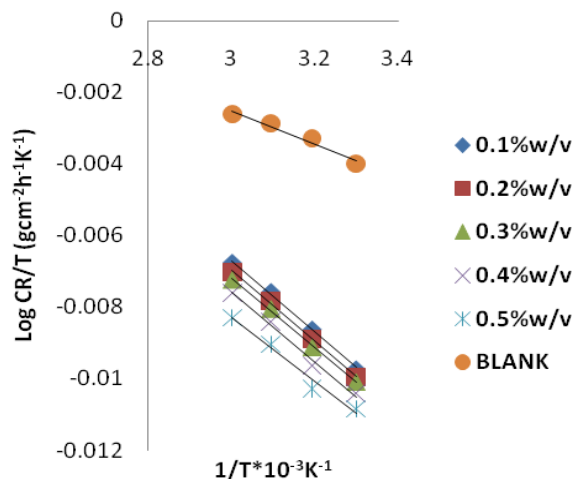$$\Delta G^*ads = -2.303RT \, \ln(55.5K_{ads}) \qquad (9)$$

Figure 13. Transition state plot for the mild steel in 5 M HCl in different concentrations of EFA and the blank.

K_{ads} is the equilibrium constant of adsorption process, R is the gas constant (8.314 $Jmol^{-1}K^{-1}$), T is temperature in Kelvin and ΔG^{o}_{ads} is the Gibb's free energy of adsorption and 55.5 is the molar concentration of water in solution. K_{ads} values for extracts of EFA was calculated from the intercepts (Figure 13) and presented in Table 4. ΔG^{o}_{ads} values were calculated using Equation 9 and also presented in Table 4. The negative values of Gibbs free energy ensures the spontaneity of adsorption process and stability of the adsorbed layer on the surface of mild steel (Shukla et al., 2011). The negative values of ΔG^{o}_{ads} of *F. asperifolia* extract indicate spontaneous adsorption of the plant extract under study onto the mild steel surface (Ahmad et al., 2010) and the strong interaction that exist between the inhibitor molecules and metal surface (Obi-Egbedi and Obot, 2008).

The values of ΔG^{o}_{ads} for *F. asperifolia* extract are below -40 KJmol^{-1} but above -20 kJmol^{-1}. This is an indication that the adsorption mechanism of the plant extract on mild steel in 5 M HCl acid solution at the temperatures 303 to 333K may be physisorption. Generally, the value of ΔG^{o}_{ads} up to -20 kJ/mol are consistent with electrostatic interaction between charged molecules and a charged metal (which indicates physical adsorption) while those more negative than -40 kJ/mol involve charge sharing or transfer from the inhibitor molecules to the metal surface to form a coordinate type of bond (which indicates chemisorption) (Bhajiwala and Vashi, 2001; Ebenso, 2003; Ahmad et al., 2010; Obi-Egbedi and Obot, 2008).

Results of the study have shown that extract of EFA inhibits the acid induced corrosion of mild steel by virtue of adsorption of its constituents onto the mild steel surface. These mechanism of adsorption observed could be attributed to the fact that EFA contains many phyto-constituents in which some have the tendency to adsorb chemically and others physically (Ating et al., 2010).

This observation may be attributed to the fact that adsorbed organic molecules can influence the behavior of electrochemical reactions involved in corrosion process in several ways. The action of organic inhibitors depends on the type of interactions between the substance and the metallic surface. The interactions can bring about a change either in electrochemical mechanism or in the surface available for the process (Ahmad et al., 2010; Obi-Egbedi and Obot, 2008).

Adsorption isotherm

Adsorption isotherms are very important to understand the mechanism of heterogenous organo-electrochemical reactions (Bockris and Khan, 1993). Adsorption of organic adsorbate at metal/solution interface can be represented by a substitutional adsorption process between organic molecules in the aqueous solution (Org $_{(sol)}$) and water molecules on the metallic surface Org$_{(ads)}$ (Langmuir, 1918; Fouda et al., 2014)

$$Org_{(sol)} + xH_2O_{(ads)} \longrightarrow Org_{(ads)} + H_2O_{(sol)}$$
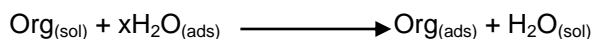
where Org $_{(sol)}$ and Org$_{(ads)}$ are the organic molecules in the aqueous solution and those adsorbed on the metallic surface respectively, $H_2O_{(ads)}$ are water molecules on metallic surface, x is the size ratio representing the number of water molecules replaced by one molecule of organic adsorbate. When equilibrium is reached, it becomes possible to obtain different expressions for the adsorption isotherm plots (Fouda et al., 2014).

These factors can be relayed to Equation (10).

$$f(\theta, x) \exp(-2a\theta) = kC \tag{10}$$

where $f(\theta, x)$ is the configurational factor which depends upon the physical model and the assumptions underlying the derivation of the isotherm, θ is the degree of surface coverage, C is the inhibitor concentration in the electrolyte, x is the size ratio, a is molecular interaction parameter and k is the equilibrium constant of the adsorption process (Eddy and Ebenso, 2008).

The surface coverage (θ) values help in understanding adsorption characteristics. The degree of surface coverage values for different concentrations of the extract of EFA obtained at different temperatures from weight loss measurement were calculated using Equation (11).

$$\text{Surface coverage } (\theta) = \% I.E/100 \tag{11}$$

Inhibition efficiency (%) is directly proportional to the fraction of the surface coverage (θ) by the adsorbed molecule. Therefore, surface coverage θ with the extract

concentration specifies the adsorption isotherm that describes the system given the relationship between the coverage of interface with the adsorbed species and the concentration of species in solution. The value of the surface coverage (θ) at different concentrations of the inhibitors in 5 M HCl solution for each extract was made to fit to various adsorption isotherms. There are many isotherm models to describe the inhibitor/metal interactions, three of these models were used namely: Langmuir, Freundlich and Temkin.

Langmuir isotherm

Langmuir adsorption isotherm describes quantitatively the formation of a monolayer adsorbate on the outer surface of the adsorbent, and after that no further adsorption takes place. The model assumes uniform energies of adsorption onto the surface and no transmigration of adsorbate in the plane of the surface.

Langmuir equation is an ideal isotherm for physical and chemical adsorption where there is no interaction between the adsorbate and the adsorbent (Eddy and Ebenso, 2008).

Assumptions of Langmuir relate the concentration of the adsorbate in the bulk of the electrolyte (C) to the degree of surface coverage (θ) according to Equation 12:

$$C_{inh}/\theta = 1/K_{ads} + C_{inh} \tag{12}$$

where C_{inh} represents the inhibitor concentration, θ is the surface coverage and K_{ads} is the adsorption equilibrium constant. The plots of C/θ against C gives a linear plot as shown in Figure 14 indicate the adsorption of the inhibitor (EFA) on the surface of mild steel is consistent with Langmuir isotherm. From the data calculated in Table 4, it's clear that Langmuir isotherm is favourable. The correlation coefficient (R^2) of the adsorption isotherm data shows that Langmuir isotherm is best fitted into the study with R^2 ranges from 0.9897 to 0.9914. The values of equilibrium constant K_{ads} are all positive, implicitly, indicative of a favourable adsorption. Similar reports were published by Nnanna et al. (2010), Mejeha et al. (2010), Akalezi et al. (2013) and Adejo et al. (2014).

Freundlich isotherm

Freundlich adsorption isotherm is commonly used to describe the adsorption characteristics for the heterogeneous surface (Hutson and Yang, 2000). The empirical equation proposed by Freundlich encompasses the heterogeneity of sites and the exponential distribution of sites and their energies (Figure 15).

Freundlich Isotherm: $\theta = K_f C^{1/n} \tag{13}$
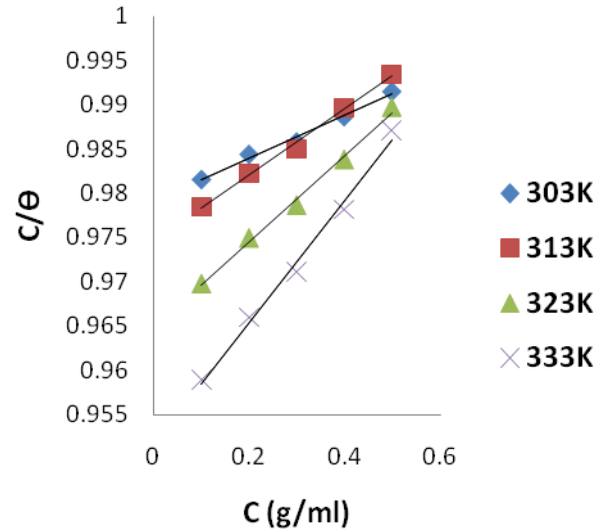

Figure 14. Langmuir adsorption isotherm for the mild steel in 5 M HCl for EFA at different temperatures.
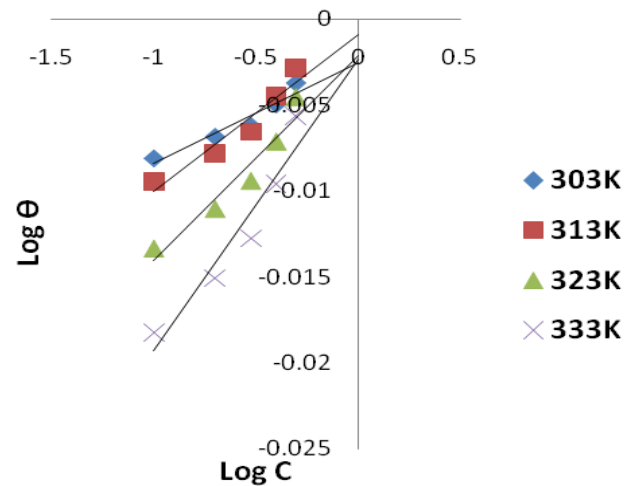
Figure 15. Freundlich isotherm for the mild steel in 5 M HCl for EFA at different temperatures.

where K_f is the Freundlich isotherm constant, n is adsorption intensity; C is the inhibitor concentration, θ is the surface coverage.

Linearizing equation 13, gives:

$$\log \theta = \log K_f + 1/n \log C \tag{14}$$

The constant K_f is an approximate indicator of adsorption capacity, while $1/n$ is a function of the strength of adsorption in the adsorption process (Weber and Chakravarti, 1974). If n = 1 then the partition between
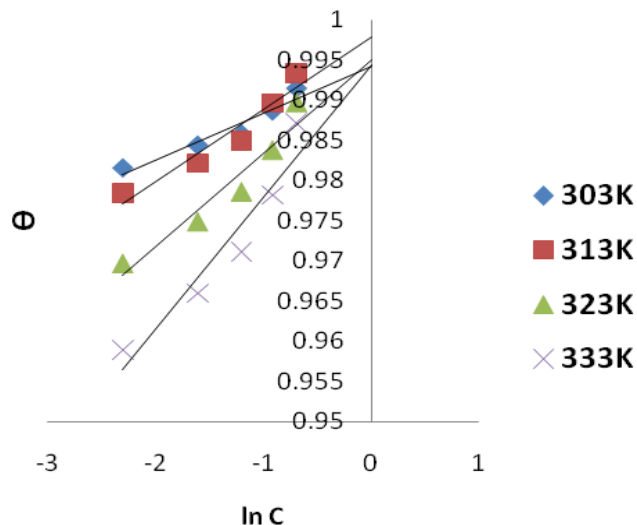
Figure 16. Temkin isotherm for the mild steel in 5 M HCl for EFA at different temperatures.

the two phases are independent of the concentration. If value of $1/n$ is below one it indicates a normal adsorption. On the other hand, $1/n$ being above one indicates cooperative adsorption (Mohan and Karthikeyan, 1997). As the temperature increases, the constants k and n change to reflect the empirical observation that the quantity adsorbed rises more slowly and higher pressures are required to saturate the surface. However, K_f and n are parameters characteristic of the sorbent-sorbate system, which must be determined by data fitting and whereas linear regression is generally used to determine the parameters of kinetic and isotherm models (Guadalupe et al., 2008). Specifically, the linear least-squares method and the linearly transformed equations have been widely applied to correlate sorption data where 1/n is a heterogeneity parameter, the smaller 1/n, the greater the expected heterogeneity. This expression reduces to a linear adsorption isotherm when 1/n = 1. If n lies between one and ten, this indicates a favorable sorption process (Goldberg, 2005). From the data in Table 5, the values of 1/n ranges from 0.0059 to 0.0169 indicating the adsorption of EFA unto the metal surfaces is favourable and the R^2 values range from 0.9178 to 0.9273.

Temkin isotherm

The Temkin isotherm equation assumes that the heat of adsorption of all the molecules in layer decreases linearly with coverage due to adsorbent-adsorbate interactions and that the adsorption is characterized by a uniform distribution of the bonding energies, up to some maximum binding energy (Temkin and Pyzhev, 1940; Oladoja et al., 2008).

The Temkin isotherm is given as:

$$\theta = b \ln A + b \ln C \qquad (15)$$

where A (l/g) is the equilibrium binding constant, corresponding to the maximum binding energy and constant b is related to the heat of adsorption. A plot of Θ against lnC (Figure 16) enables the determination of the isotherm constants B and A from the slope and the intercept of the linear plot. The Temkin equilibrium adsorption plot relates the mild steel and the liquid phase concentration of HCl at equilibrium.

The values of b calculated are between 9.8673 and 9.9517 for EFA as shown in Table 5. The regression values of the extract tend towards unity (Oladoja et al., 2008; Adejoet al., 2014).

Conclusion

This study has shown that ethanolic extract of *F. asperifolia* as well as its fractions (n-hexane, ethyl acetate, butanol and aqueous) are found to be effective corrosion inhibitors for mild steel in acidic medium. The reaction was found to best obey Langmuir adsorption isotherm from the fit of the experimental data at all concentrations and temperature ranges studied.

Conflict of Interests

The authors have not declared any conflict of interests.

ACKNOWLEDGEMENTS

REFERENCES

Abdulrahman AS, Ismail M, Sakhawat HM (2011). Inhibition of corrosion of mild steel in hydrochloric acid by *Bambusa arundinacea*. Int. Rev. Mech. Eng. 5(1):59–63.

Adejo SO, Ekwenchi MM, Gbertyo JA, Menenge T, Ogbodo JO (2014). Determination of adsorption Isotherm model best fit for methanol leaf extract of *Securinega virosa* as corrosion inhibitor for corrosion of mild steel in HCl. J. Adv. Chem. 10(5):2737-2742. ISSN 2321-807X.

Adjanohoun JC, Aboubakar N, Dramane K, Ebot ME, Ekpere JA, Enow-Orock EG (1996). Traditional medicine and pharmacopoeia in contribution to ethnobotanical and floristic studies in Cameroon, Ife press, Nigeria. pp. 301-325.

Afidah AR, Kassim J (2008). Recent development of vegetal tannins in corrosion protection of iron and steel. Recent Patents Mater. Sci. 1:223-231.

Ahmad I, Prasad R, Quraishi MA (2010). Inhibition of mild steel corrosion

in acid solution by Pheniramine drug: Experimental and theoretical study. Corros. Sci. 52:3033-3341.

Akalezi CO, Enenebaku CK, Oguzie EE (2013). Inhibition of acid corrosion of mild steel by biomass extract from the *Petersianthus macrocarpus* plant. J. Mater. Environ. Sci. 4(2):217-226.

Al-Otaibi MS, Al-Mayouf AM, Khan M, Mousa AA, Al-Mazroa SA, Alkhathlan HZ (2012). Corrosion inhibitory action of some plant extracts on the corrosion of mild steel in acidic media. Arabian J. Chem. 7(3):340–346.

Al-qudah MA (2011). Inhibition of Copper Corrosion by Flavonoids in Nitric Acid. E-J. Chem. 8(1):326-332.

Anauda L, Sathiyanathan RA, Maruthamuthu SB, Selvanayagam MC, Mohanan SB, Palaniswamy NB (2005). Corrosion inhibition of mild steel by ethanolic extracts of *Ricinus communis* leaves. Indian J. Chem. Technol. 12(3):356-360.

Ansari A, Znini M, Hamdani I, Majidi L, Bouyanzer A, Hammouti B (2014). Experimental and theoretical investigations anti-corrosive properties of Menthone on mild steel corrosion in hydrochloric acid. J. Mater. Environ. Sci. 5(1):81-94.

Ashassi-Sorkhabi H, Masoumi B, Ejbari P, Asghari E (2009). Corrosion inhibition of mild steel in acidic media by Basic yellow 13 dye. J. Appl. Electrochem. 39(9):1497-1501.

Ating EI, Umoren SA, Udousoro II, Ebenso EE, Udoh AP (2010). Leaves extract of *Ananas sativum* as green corrosion inhibitor for aluminium in hydrochloric acid solutions. Green Chem. Lett. Rev. 3(2):61-68.

Awad MI (2006). Eco friendly corrosion inhibitors: Inhibitive action of quinine for corrosion of low carbon steel in 1M HCl. J. Appl. Electrochem. 36:1163-1168.

Behpour M, Mohammadi N (2012). Investigation of inhibition properties of aromatic thiol self-assembled monolayer for corrosion protection. Corros. Sci. 65 (2012):331–339.

Bendahou MA, Benadellah MBE, Hammouti BB (2006). A study of rosemary oil as a green corrosion inhibitor for steel in 2M H_3PO_4. Pigment Resin Technol. 35(2):95-110.

Bhajiwala HM, Vashi RT (2001). Ethanolamine, diethanolamine and triethanolamine as corrosion inhibitor for zinc in binary acid mixture ($HNO_3 + H_3PO_4$). Bull. Electrochem. 17:441-448.

Blaedel WJ, Meloche VW (1963). Elementary quantitative analysis, theory and practice. Row, Peterson UK. P. 562.

Bockris JOM, Khan SUM (1993). Surface Electrochemistry: A molecular level approach. Plenum: New York.

Bouklah M, Hammouti B, Lagrenee M, Bentiss F (2006). Thermodynamic properties of 2, 5 –bis (4-methoxy phenyl) -1, 3, 4-oxadiazole as a corrosion inhibitor for mild steel in normal sulfuric acid medium. Corros. Sci. 48(9):2831-2842.

Chen A, Cao F, Liao X, Liu W, Zheng L, Zhang J, Cao C (2013). Study of pitting corrosion on mild steel during wet-dry cycles by electrochemical noise analysis based on chaos theory. Corros. Sci. 66:183–195.

Dahmani M, Et-Touhami A, Al-Deyab SS, Hammouti B, Bouyanzer A (2010). Corrosion inhibition of C38 steel in 1M HCl: A comparative Study of Black Pepper Extract and its isolated piperine. Int. J. Electrochem. 5:1060-1069.

Dauda KT, Atasie VN, Adetimilehin AA (2013). Kinetic of the inhibitory effects of Ethanolic Extracts of *Vernonia amydgalina* on the Corrosion of Aluminium in 1.0M HCl. Chem. J. 3(3):86-89.

De Sauza FS, Spinelli A (2009). Caffeic acid as a green corrosion inhibitor for mild steel. Corros. Sci. 51(3):642-649.

Devarayan K, Mayakrishnan G, Nagarajan S (2012). Green Inhibitors for Corrosion of Metals: A Review. Chem. Sci. Rev. Lett. 1(1):1-8. ISSN 2278-6783.

Ebenso EE (2003). Synergistic effect of halide ions on the corrosion inhibition of aluminium in H_2SO_4 using 2-acetylphenothiazine. Mater. Chem. Phys. 79(1):58-70.

Ebenso EE, Eddy NO, Odiongenyi AO (2008). Corrosion inhibitive properties and adsorption behaviour of ethanol extract of Piper guinensis as a green corrosion inhibitor for mild steel in H_2SO_4 . Afr. J. Pure Appl. Chem. 2(11):107-115.

Eddy NO, Ebenso EE (2008). Adsorption and inhibitive properties of ethanol extracts of *Musa sapientum* peels as a green corrosion inhibitor for mild steel in H_2SO_4. Afr. J. Pure Appl. Chem.

2(6):046-054.

Fouda AS, Tawfik H, Badr AH (2009). Corrosion inhibition of mild steel by *Camellia sinensis* extract as green inhibitor. Adv. Mater. Corros. 1:1-7.

Fouda AS, Tawfik H, Badr AH (2012). Corrosion inhibition of mild steel by *Camellia sinensis* extract as green inhibitor. Adv. Mater. Corrosion. 1:1-7.

Fouda AS, Elewady GY, Shalabi K, Habbouba S (2014). *Punica* plant extract as green corrosion inhibitor for C-steel in hydrochloric acid solutions. Int. J. Electrochem. Sci. 9:4866-4883.

Goldberg S (2005). Equations and Models describing Adsorption Processes in Soils. Chemical Processes in Soils. SSSA Book Series. 2005:8.

Guadalupe R, Reynel-Avila HE, Bonilla-Petriciolet A, Cano-Rodriguez C, Velasco-Santos C Martinez-Hernandez AL (2008). Recycling poultry feathers for Pb removal from wastewater: kinetic and equilibrium studies. Proceedings World Academy Sci. Eng. Technol. 2008:30.

Hutson ND, Yang RT (2000). Adsorption. J. Colloid Interf. Sci. P. 189.

Ismail M, Abdulrahman AS, Hussain MS (2011). Solid waste as environmental benign corrosion inhibitors in acid medium. Int. J. Eng. Sci. Technol. 3(2):1742-1748.

James AO, Akaranta O (2009). Corrosion inhibition of aluminum in 2.0M hydrochloric acid solution by the acetone extract of red onion skin. Afr. J. Pure Appl. Chem. 3(12):262-268.

Ji G, Shukla SK, Dwivedi P, Sundaram S, Ebenso EE, Prakash R (2012). *Parthenium hysterophorus* Plant Extract as an Efficient Green Corrosion Inhibitor for Mild Steel in Acidic Environment. Int. J. Electrochem. Sci. 7:9933-9945.

Johnsirani V, Sathiyabama J, Rajendran S, Prabha S (2012). Inhibitory Mechanism of Carbon Steel Corrosion in Sea Water by an Aqueous Extract of Henna leaves. Int. Sch. Res. Net. 2012:574321. Doi:10.5402/2012/574321.

Khadom AA, Yaro AS, Kadum AH (2010). Corrosion inhibition by naphthylamine and phenylenediamine for the corrosion of copper–nickel alloy in hydrochloric acid. J. Taiwan Ins. Chem. Eng. 41(1):122-125.

Lagrenee M, Mernari B, Bouanis M, Traisnel M, Bentiss F (2002). Study of the mechanism and inhibiting efficiency of 3,5-bis(4-methylthiophenyl)-4H-1,2,4-triazole on mild steel corrosion in acidic media. Corrosion Sci. 44(2002):573-588.

Langmuir I (1918). The adsorption of gases on plane surfaces of glass, mica and platinum. J. Am. Chem. Soc. 40:1362-1403.

Loto CA (1998). The effect of bitter leaf extracts on corrosion of mild steel in 0.5 M HCl and H_2SO_4 solutions. Nig. Corrosion J. Int. 1:19-20.

Loto CA, Etete PL, Popoola API (2011). Inhibition effect of Kola tree and Tobacco extracts on the corrosion of Austenitic stainless steel in acid chloride environment. Int. J. Electrochem. Sci. 6:4876-4890.

Mejeha IM, Uroh AA, Okeoma KB, Alozie GA (2010). The inhibitive effect of *Solanum melongena* L. leaf extract on the corrosion of aluminium in tetraoxosulphate (VI) acid. Afr. J. Pure Appl. Chem. 4(8):158-165.

Mercer AD (1985). Test methods of corrosion inhibitors Br. Corrosion J. 20(2):61.

Mohan S, Karthikeyan J (1997). Removal of lignin and tannin color from aqueous solution by adsorption on to activated carbon solution by adsorption on to activated charcoal, Environ. Pollution. 97:183-187.

Musa AY, Khadom AA, Kadhum AH, Mohamad AB, Takriff MS (2010). Kinetic behavior of mild steel corrosion inhibition by 4-amino-5-phenyl-4H-1, 2, 4-trizole-3-thiol. Journal of Taiwan institute of chemical engineers 41(2010) 126–128. J. Taiwan Ins. Chem. Eng. 41:126.

Negm NA, Kandile NG, Badr EA, Mohammed MA (2012). Gravimetric and electrochemical evaluation of environmentally friendly non-ionic corrosion inhibitors for carbon steel in 1 M HCl. Corrosion Sci. 65:94–103.

Nkuzinna O, Menkiti MC, Onukwuli OD (2011). Inhibition of Copper Corrosion by Acid extracts of *Gnetum africana* and *Musa acuminate* peel. Int. J. Multidisciplinary Sci. Eng. 2(5):2045-7057.

Nnanna LA, Onwuagba BN, Mejeha IM, Okeoma KB (2010). Inhibitory effects of some plant extracts on the acid corrosion of aluminium alloy. Afr. J. Pure Appl. Chem. 4(1):011-016.

Obi-Egbedi NO, Obot IB (2010). Adsorption behavior and corrosion

inhibitive potential of xanthine on mild steel/sulphuric acid interface, Arabian J. Chem. 5:121–133.

Obi-Egbedi NO, Obot IB (2008a). Inhibitory effect and adsorption characteristics of 2,3-Diaminonaphthalene at Aluminum/Hydrochloric acid interface: Experimental and theoretical study. Surf. Rev. Lett. 15(6):903.

Oguzie EE (2008). Corrosion inhibitive effect and adsorption Behaviour of *Hibiscus sabdariffa* extract on mild steel in acidic media. Portugaliae Electrochimica Acta. 26:303–314.

Oguzie E, Onuoha G, Onuchukwu A (2004). Influence of halide ions on inhibitive effect of congo red dye on the corrosion of mild steel in sulphuric acid solution. Mater. Chem. Phys. 89:305.

Okafor PC, Ebenso EE, Ekpe UJ (2010). *Azadirachta indica* extracts as corrosion inhibitor for mild steel in acid medium. Int. J. Electrochem. Sci. 5(7):978–993.

Okafor PC, Ebiekpe VE, Azike CF, Egbung GE, Brisibe EA, Ebenso EE (2012). Inhibitory action of *Artemisia annua* on the corrosion of mild steel in H_2SO_4 solution. Int. J. Corrosion pp. 1-8.

Oladoja NA, Aboluwoye CO, Oladimeji YB (2008). Kinetics and isotherm studies on methylene blue adsorption onto ground palm kernel coat. Turkish J. Eng. Environ. Sci. 32:303-312.

Olasehinde EF, Olusegun SJ, Adesina AS, Omogbehin SA, Momoh-Yahayah H (2013). Inhibitory Action of *Nicotiana tabacum* Extracts on the Corrosion of Mild Steel in HCl: Adsorption and Thermodynamics Study. Nat. Sci. 11(1):83-90.

Olusegun SJ, Adeiza BA, Ikeke KI, Bodunrin MO (2013). Jatropha Curcas Leaves Extract as Corrosion Inhibitor for Mild Steel in 1M Hydrochloric Acid. J. Emerging Trends Eng. Appl. Sci. (JETEAS) 4(1):138-143 ISSN: 2141-7016.

Omoniwa BP, Luka CD (2012). Antidiabetic and toxicity evaluation of aqueous stem extract of *Ficus asperifolia* in normal and alloxan-induced diabetic albino rats. J. Exp. Biol. Sci. 3(4):726-732.

Onyeka EU, Nwabekwe IO (2007). Phytochemical profile of some green leafy vegetable in S.E. Ngeria. Nigerian Food J. 25(1):67–76.

Owate IO, Nwadiuko OC, Dike II, Isu JO, Nnanna LA (2014). Inhibition of mild steel corrosion by *Aspilia Africana* in acidic solution. Am. J. Mater. Sci. 4(3):144-149.

Popova A, Sokolova E, Raicheva S, Christov M (2003). AC and DC study of the temperature effect on mild steel corrosion in acid media in the presence of benzimidazole derivatives. Corrosion Sci. 45:33-58.

Rengamani S, Muralidharan S, Kulandainathan MA, Iyer SV (1994). Inhibiting and accelerating effects of aminophenols on the corrosion and permeation of hydrogen through mild steel in acidic solutions. J. Appl. Electrochem. 24:355-360.

Schmitt G (1984). Application of inhibitors for acid media: Report prepared for the European Federation of Corrosion Working Party on Inhibitors. Br. Corros. J. 19(4):165-176.

Sherine B, Abdul Nasser AJ, Rajendran S (2010). Inhibitive action of hydroquinone-Zn^{2+} system in controlling the corrosion of carbon steel in well water. Int. J. Eng. Sci. Technol. 2(4):341–357.

Shukla SK, Quraishi MA (2009). 4-substituted anilinomethylpropionate: New and efficient corrosion inhibitors for mild steel in hydrochloric acid solution. Corrosion Sci. 51:1007.

Shukla SK, Quraishi MA, Ebenso EE (2011). Adsorption and corrosion inhibition properties of Cefadroxil on mild steel in hydrochloric acid. Int. J. Electrochem. Sci. 6:2912-2931.

Singh AK, Quraishi MA (2010). Effect of Cefazolin on the corrosion of Mild steel in HCl solution. Corrosion Sci. 52:152-160.

Tao Z, Zhang S, Li W, Hou B (2009). Corrosion inhibition of mild steel in acidic solution by some oxo-triazole derivatives. Corrosion Sci. 51(11):2588-2595.

Temkin MI, Pyzhev V (1940). Kinetic of ammonia synthesis on promoted iron catalyst. Acta physiochim. URSS. 12:327-356.

Ten KW, Kassim MJ, Oo CW (2012). Possible improvement of catechin as corrosion inhibitor in acidic medium. Corrosion Sci. 65:152–162.

Umoru LE, Fawehinmi IA, Fasasi AY (2006). Investigation of the inhibitive influence of *Theobroma cacao* and *Cola acuminate* leaves extracts on the corrosion of mild steel in sea water. J. Appl. Sci. Res. 2(4):200-204.

Vijayalakshmi PR, Rajalakshmi R, Subhashini S (2011). Corrosion inhibition of aqueous extract of *Cocos nucifera* – Coconut Palm-Petiole extract from destructive distillation for the corrosion of mild steel in acidic medium. Portugaliiae Electrochimica Acta. 29(1):9-21.

Villamil RFV, Corio P, Rubin JC, Agostinho SMI (1999). Effect of sodium dodecylsulfate on copper corrosion in sulfuric acid media in the absence and presence of benzotriazole. J. Electroanal. Chem. 472:112–119.

Wagenen BC, Larsen R, Cardellina JH, Ran dazzo D, Lidert ZC, Swithenbank C (1993). Ulosantoin, a potent insecticide from the sponge Ulosa ruetzleri. J. Org. Chem. 58:335-337.

Weber TN, Chakravarti RK (1974). Pore and solid diffusion models for fixed bed adsorbers. J. Am. Inst. Chem. Eng. 20:228-238.

African Journal of Pure and Applied Chemistry

Related Journals Published by Academic Journals

- *African Journal of Mathematics and Computer Science Research*
- *International Journal of the Physical Sciences*
- *Journal of Geology and Mining Research Technology*
- *Journal of Environmental Chemistry and Ecotoxicology*
- *Journal of Internet and Information Systems*
- *Journal of Oceanography and Marine Science*
- *Journal of Petroleum Technology and Alternative Fuels*